A complex relation between levels of adult hippocampal neurogenesis and expression of the immature neuron marker doublecortin

I. Mendez-David, Denis J. David, Claudine Deloménie, Laurent Tritchler, Jean Martin Beaulieu, Romain Colle, Emmanuelle Corruble, Alain Michel Gardier, Renté É. Hen

▶ **To cite this version:**

I. Mendez-David, Denis J. David, Claudine Deloménie, Laurent Tritchler, Jean Martin Beaulieu, et al.. A complex relation between levels of adult hippocampal neurogenesis and expression of the immature neuron marker doublecortin. Hippocampus, 2023, 33 (10), pp.1075-1093. 10.1002/hipo.23568 . hal-04271280

HAL Id: hal-04271280
https://hal.science/hal-04271280

Submitted on 15 Nov 2023

HAL is a multi-disciplinary open access archive for the deposit and dissemination of scientific research documents, whether they are published or not. The documents may come from teaching and research institutions in France or abroad, or from public or private research centers.

L'archive ouverte pluridisciplinaire **HAL**, est destinée au dépôt et à la diffusion de documents scientifiques de niveau recherche, publiés ou non, émanant des établissements d'enseignement et de recherche français ou étrangers, des laboratoires publics ou privés.

Distributed under a Creative Commons Attribution 4.0 International License

Check for updates

Received: 25 August 2022 | Revised: 8 May 2023 | Accepted: 20 June 2023

DOI: 10.1002/hipo.23568

RESEARCH ARTICLE

WILEY

A complex relation between levels of adult hippocampal neurogenesis and expression of the immature neuron marker doublecortin

Indira Mendez-David[1,2,3] | Denis Joseph David[1,2,3] | Claudine Deloménie[4] | Laurent Tritchler[1] | Jean-Martin Beaulieu[5] | Romain Colle[6,7] | Emmanuelle Corruble[6,7] | Alain Michel Gardier[1] | René Hen[2,3]

[1]Université Paris-Saclay, UVSQ, Centre de recherche en Epidémiologie et Santé des Populations (CESP), UMR 1018, CESP-Inserm, Team Moods, Faculté de Pharmacie, Bâtiment Henri MOISSAN, Orsay, France

[2]Department of Psychiatry, Columbia University, New York, New York, USA

[3]Division of Integrative Neuroscience, New York State Psychiatric Institute, New York, New York, USA

[4]UMS-IPSIT ACTAGen, Inserm, CNRS, Ingénierie et Plateformes au Service de l'Innovation Thérapeutique, Université Paris-Saclay, Bâtiment Henri MOISSAN, Orsay, France

[5]Department of Pharmacology and Toxicology, University of Toronto, Toronto, Ontario, Canada

[6]CESP, MOODS Team, INSERM UMR 1018, Faculté de Médecine, Univ Paris-Saclay, Le Kremlin Bicêtre, France

[7]Service Hospitalo-Universitaire de Psychiatrie de Bicêtre, Hôpitaux Universitaires Paris-Saclay, Assistance Publique-Hôpitaux de Paris, Hôpital de Bicêtre, Le Kremlin Bicêtre, France

Correspondence
Indira Mendez-David and Denis Joseph David, Université Paris-Saclay, UVSQ, UMR 1018, CESP-Inserm, Team MOODS, Faculté de Pharmacie, Bâtiment Henri MOISSAN, 17, avenue des Sciences, F-91400 Orsay, France.
Email: indira.david@universite-paris-saclay.fr and denis.david@universite-paris-saclay.fr

René Hen, Department of Psychiatry, Columbia University, New York, NY, USA.
Email: rh95@cumc.columbia.edu

Funding information
Fondation Pierre Deniker pour la Recherche et la Prévention en Santé Mentale; National Alliance for Research on Schizophrenia and Depression, Grant/Award Number: YoungInvestigatorAward2017toIndiraMendez-David

Abstract

We investigated the mechanisms underlying the effects of the antidepressant fluoxetine on behavior and adult hippocampal neurogenesis (AHN). After confirming our earlier report that the signaling molecule β-arrestin-2 (β-Arr2) is required for the antidepressant-like effects of fluoxetine, we found that the effects of fluoxetine on proliferation of neural progenitors and survival of adult-born granule cells are absent in the β-Arr2 knockout (KO) mice. To our surprise, fluoxetine induced a dramatic upregulation of the number of doublecortin (DCX)-expressing cells in the β-Arr2 KO mice, indicating that this marker can be increased even though AHN is not. We discovered two other conditions where a complex relationship occurs between the number of DCX-expressing cells compared to levels of AHN: a chronic antidepressant model where DCX is upregulated and an inflammation model where DCX is downregulated. We concluded that assessing the number of DCX-expressing cells alone to quantify levels of AHN can be complex and that caution should be applied when label retention techniques are unavailable.

KEYWORDS
adult hippocampal neurogenesis, antidepressant, doublecortin, inflammation, β-arrestin-2

Indira Mendez-David and Denis Joseph David are co-first authors.

 © 2023 Wiley Periodicals LLC.

1 | INTRODUCTION

In the adult mammalian brain, there are two regions where new neurons are generated until old age, the subventricular zone (SVZ), which gives rise to neurons that migrate to the olfactory bulb, and the subgranular zone (SGZ) of the hippocampus, which gives rise to adult-born granule cells localized in the dentate gyrus (DG). In mice, both the SVZ and SGZ neural stem cell niches give rise to new neurons until old age although the numbers decrease significantly with age (for review; Snyder, 2019). In primates, including humans, the SVZ niche produces young neurons until about 1 year of age, after which neurogenesis becomes undetectable (Sanai et al., 2011); in contrast, the SGZ niche keeps producing young neurons considerably later; however, there is currently a controversy as to how long the human SGZ keeps producing young neurons. Most reports indicate that adult-born granule cells are generated until old age (Boldrini et al., 2018; Boldrini et al., 2019b; Flor-Garcia et al., 2020; Tartt et al., 2018; Zhou et al., 2022), but a few reports suggest that the production of young neurons becomes negligible in humans after adolescence (Franjic et al., 2022; Sorrells et al., 2018). This controversy may be partially due to experimental conditions (such as post-mortem intervals as well as tissue conservation and fixation; Flor-Garcia et al., 2020) but also to the fact that there are few markers of young neurons that have been studied in the human brain (Mendez-David et al., 2022); most studies have used doublecortin (DCX) and as we show in the current study the number of DCX-expressing cells is not always a good estimate of the number of adult-born neurons.

In rodents, adult hippocampal neurogenesis (AHN) has been implicated in a range of cognitive functions, as well as mood and anxiety-related behaviors. Notably, studies have shown that some of the effects of antidepressants, such as Selective Serotonin Reuptake Inhibitors, require neurogenesis in the DG (David et al., 2009; Lino de Oliveira et al., 2020; Santarelli et al., 2003). The SSRI fluoxetine has been shown to stimulate several stages of the neurogenesis process: proliferation of the transit amplifying cells, survival of the young adult-born granule cells, and differentiation of these young granule cells into mature granule cells (Encinas et al., 2006; Malberg et al., 2000). The mechanisms underlying these effects are only partially understood; activation of several serotonin receptors, including the 5-HT_{1A}, 5-HT_4, 5-HT_{5A}, and 5-HT_{2A} receptors, appears to be important as well as an increase in Brain-Derived Neurotrophic Factor and the resulting activation of the Trk-B receptor (David et al., 2009; Kobayashi et al., 2010; Ma et al., 2017; Sagi et al., 2019). There is also some evidence indicating that the signaling molecule β-arrestin-2 (β-Arr2), which operates downstream of a number of G-protein coupled receptors (such as 5-HT_4 and 5-HT_{2A} receptors), is involved in mood disorders and plays a role in the action of antidepressants (Asth et al., 2016; Beaulieu et al., 2008; David et al., 2009). In the current study, we investigated the contribution of β-Arr2 to the effects of the antidepressant fluoxetine and discovered a surprising effect of fluoxetine on the expression of doublecortin, a commonly used marker for young adult-born granule cells in the DG.

2 | MATERIALS AND METHODS

2.1 | Contact for reagent and resource sharing

Resources and reagents used for this study are described in Table 1. Further information and requests for material and methods should be directed to and will be fulfilled by the lead contacts, Denis Joseph David (denis.david@universite-paris-saclay.fr) or René Hen (rh95@cumc.columbia.edu).

2.2 | Experimental model and subject details

All mice were 7–8 weeks old, weighed 23–25 g at the beginning of the treatment, and were maintained on a 12 h light:12 h dark schedule (lights on at 0600). They were housed in groups of five. Food and water were provided ad libitum. All testing was in conformity with the institutional guidelines that are in compliance with national and international laws and policies (Council directive # 87-848, October 19, 1987, Ministère de l'Agriculture et de la Forêt, Service Vétérinaire de la Santé et de la Protection Animale; NIH Guide for the Care and Use of Laboratory Animal) and in compliance with protocols approved by the Institutional Animal Care and Use Committee (CEE26 authorization #4747-2016033116126273 at Université Paris-Saclay; Institutional Animal Care and Use Committee of Columbia University and the Research Foundation for Mental Hygiene, Inc.).

2.3 | Animals

2.3.1 | Study in β-Arr2 knockout mice

β-Arr2 heterozygous mice were provided by Robert Lefkowitz (Duke University). Male heterozygous β-Arr2 heterozygous female mutant β-Arr2 mice (age 4–6 months) were bred on a mixed S129/Sv × C57BL/6 genetic background at the University Paris-Saclay's animal facility. Resulting pups were genotyped by polymerase chain reaction (Beaulieu et al., 2008; David et al., 2009). Male heterozygous β-Arr2 Hets, β-Arr2 knockout (KO), and their wild-type (WT) littermates, 25–30 g body weight, were used to test the behavioral and neurogenic effects of a chronic treatment with fluoxetine (18 mg/kg/day) (see timeline of experiments in Figure 1a).

2.3.2 | Study in CORT model

Study in mice presenting an intact AHN

Male C57BL/6JRj mice (Janvier Labs; 25–30 g body weight) were used to test the neurogenic effects of a chronic treatment with fluoxetine (18 mg/kg/day) in the CORT model (see timeline of experiments in Figure 3a or Figure 6a).

10981063, 2023, 10, Downloaded from https://onlinelibrary.wiley.com/doi/10.1002/hipo.23568 by Université de Versailles-Saint-Quentin-en-Yvelines, Wiley Online Library on [15/11/2023]. See the Terms and Conditions (https://onlinelibrary.wiley.com/terms-and-conditions) on Wiley Online Library for rules of use; OA articles are governed by the applicable Creative Commons License

2.3.3 | Study in irradiated mice

Male C57BL/6Ntac mice (Taconic Farms, 25–30 g body weight) were used to test the neurogenic effects of a chronic treatment with fluoxetine (18 mg/kg/day) in the CORT model after x-ray procedure (see timeline of experiments in Figure 4a).

2.3.4 | Study in GFAP-TK+ mice

Transgenic GFAP-TK+ and transgenic GFAP-TK− mice were used to test the neurogenic effects of a chronic treatment with fluoxetine (18 mg/kg/day in the drinking water) in the CORT model (Mendez-David et al., 2017; Schloesser et al., 2009; Snyder et al., 2011) (see timeline of experiments in Figure 4a). An agreement (license L-O 15-2015/0) between the NIH and the Université Paris-Saclay provides UMR 1018, CESP-Inserm laboratory, with the use of transgenic GFAP-TK mice, which was developed in the laboratory of Dr Heather Cameron of the National Institute of Mental Health (NIMH).

2.3.5 | Lipopolysaccharide study

Male C57BL/6JRj mice (Janvier Labs, 25–30 g body weight) locally injected in the dorsal DG with Lipopolysaccharide were used to assess

TABLE 1 Key resources table for material and methods.

Reagent or resource	Source	Identifier
Antibodies		
Anti-mouse 5-Bromo-2-Deoxyuridine (BrdU)	BD Biosciences	Cat#347580
Anti-rat BrdU	Serotec	Cat#MCA2060
Anti-goat-doublecortin (DCX)	Santa Cruz Biotechnology	Cat#SC8066
Anti-rabbit-KI67	Eurobio	Cat#VP-RM04
Anti-rabbit-calretinin	Swant	Cat#7699/3H
Anti-mouse neuronal-specific nuclear protein (NeuN)	Chemicon	Cat#MAB377
Biotinylated anti-mouse IgG (H + L)	Vector	Cat#BA9200
Biotin SP-conjugated Donkey anti-rat	Jackson ImmunoResearch	Cat#712-065-150
Biotin SP conjugated Donkey anti-goat IgG (H + L)	Jackson ImmunoResearch	Cat#705-065-003
CY2 conjugated Streptavidin	Jackson ImmunoResearch	Cat#016-220-084
Donkey anti-goat CY3	Jackson ImmunoResearch	Cat#705-165-003
Donkey anti-mouse CY5	Jackson ImmunoResearch	Cat#715-605-150
miScript® II RT Kit	Qiagen	Cat#218161
miScript® SYBR® Green PCR Kit	Qiagen	Cat#218073
Chemicals, peptides, and recombinant proteins		
hydroxypropyl-β-cyclodextrin	Roquette	Cat#965440
Corticosterone	Sigma-Aldrich	Cat#C2505
Valganciclovir	Sigma-Aldrich	Cat#PHR1626-1g
Lipopolysaccharide	Sigma-Aldrich	Cat#L2630
Fluoxetine	Anawa	Cat#BG0197
TRIzol® Reagent	Invitrogen	Cat#15596026
Experimental models: organisms/strains		
β-arrestin-2 +/−	Bob J. Lefkowitz (Duke University)	
β-arrestin-1 +/−	J. M. Beaulieu (University of Toronto)	
GFAP-TK+	Cameron H, NIMH, (license L-O 15-2015/0)	
C57BL/6JRj	Janvier Labs	
C57BL/6Ntac	Taconic Farms	
Software and algorithms		
Prism 8.0	GraphPad	
EPM3C	Bioseb	
Anymaze 6	Stoelting	

(Continues)

10981063, 2023, 10, Downloaded from https://onlinelibrary.wiley.com/doi/10.1002/hipo.23568 by Université de Versailles-Saint-Quentin-en-Yvelines, Wiley Online Library on [15/11/2023]. See the Terms and Conditions (https://onlinelibrary.wiley.com/terms-and-conditions) on Wiley Online Library for rules of use; OA articles are governed by the applicable Creative Commons License

TABLE 1 (Continued)

Reagent or resource	Source	Identifier
Apparatus		
Open field	Vivo Tech/Ugo Basile	
Elevated plus maze	Bioseb	
Cranial irradiation	PXI-X-RAD	

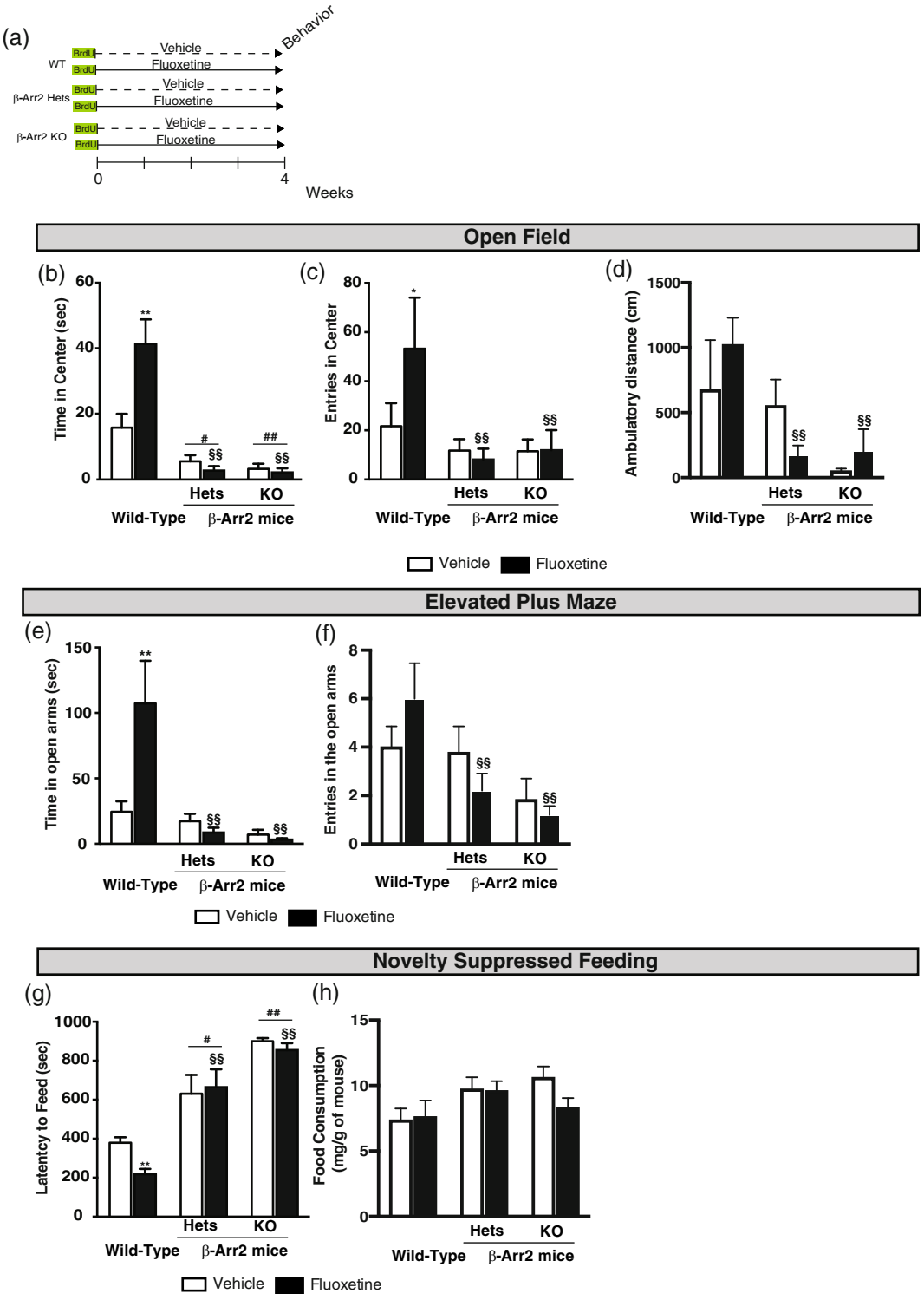

FIGURE 1 Legend on next page.

10981063, 2023, 10, Downloaded from https://onlinelibrary.wiley.com/doi/10.1002/hipo.23568 by Université de Versailles-Saint-Quentin-en-Yvelines, Wiley Online Library on [15/11/2023]. See the Terms and Conditions (https://onlinelibrary.wiley.com/terms-and-conditions) on Wiley Online Library for rules of use; OA articles are governed by the applicable Creative Commons License

the role of inflammation on AHN (see timeline of experiments in Figure 5a).

2.4 | Drugs and treatment

2.4.1 | Study in β-Arr2 KO mice

Behavioral and neurogenic effects of a 4-week treatment with fluoxetine hydrochloride (Anawa Trading, 160 mg/mL, equivalent to 18 mg/kg/day in drinking water, according to David et al. (2009)) were tested in male β-Arr2 Hets, β-Arr2 KO mice and their WT littermates (Figures 1 and 2, Figure S2). Similarly, neurogenic effects of a 4-week fluoxetine treatment were evaluated in male β-arrestin-1 (β-Arr1) KO mice and their littermates (Figure S1).

2.4.2 | Study in CORT model

Corticosterone (4-pregnen-11b-DIOL-3 20-DIONE 21-hemisuccinate [35 μg/mL]) purchased from Sigma-Aldrich was dissolved in a vehicle (0.45% hydroxypropyl-β-cyclodextrin (β-CD); Sigma-Aldrich). Fluoxetine hydrochloride (160 mg/mL, equivalent to 18 mg/kg/day) was purchased from Anawa Trading and dissolved in 0.45% β-CD/corticosterone solution. Corticosterone-treated water was changed every 3 days to prevent any possible degradation as previously described (David et al., 2009; Mendez-David et al., 2014). Fluoxetine (18 mg/kg/day drinking water) was administered chronically to mice for 28 days, 4 weeks after chronic corticosterone, and their effects on AHN were observed in mice presenting an intact (Figures 3 and 6, Figure S3) or an ablation of AHN (Figure 4, Figure S4).

2.4.3 | Arresting adult hippocampal neurogenesis

X-irradiation

Male C57BL/6Ntac mice were anesthetized with ketamine and xylazine (75/20 mg/kg), placed in a stereotaxic frame, and exposed to cranial irradiation using a PXI X-RAD 320 X-ray system operated at 300 kV and 12 mA with a 2-mm Al filter according to a well-described procedure (Anacker et al., 2018; Mendez-David et al., 2014). Animals were protected with a lead shield that covered the entire body, but left unshielded by a $3.22 \times 11\ mm^2$ treatment field above the hippocampus (interaural 3.00 to 0.00) exposed to x-ray, thus effectively preventing irradiation from targeting the rest of the brain (Santarelli et al., 2003). The corrected dose rate was approximately 0.95 Gy per min at a source-to-skin distance of 36 cm. The procedure lasted 2 min 39 s, delivering a total of 2.5 Gy. Three 2.5 Gy doses were delivered on Days 1, 4, and 7. This 7.5 Gy cumulative dose was determined from prior pilot experiments to be the minimum dosage necessary to result in permanent ablation of adult-born neurons in the DG as assessed by expression of the immature neuronal marker doublecortin. The reason for using a fractionated paradigm rather than a single high dose of 7.5 Gy is that the ablation is not permanent after a single high dose. Then, Sham or Irradiated animals were submitted to the CORT protocol in the presence of fluoxetine (18 mg/kg/day in the drinking water during the last 4 weeks) and killed 8 weeks after.

Genetic ablation of AHN study

To arrest neurogenesis in GFAP-Tk+ mice, ValGanciclovir (vGCV, Sigma-Aldrich the L-valyl ester of ganciclovir—were given to GFAP-Tk + mice and their littermates GFAP-Tk− from Monday to Friday during 12 weeks through the animals' chow at a concentration of 165 mg/kg (SSNIFF; Mendez-David et al., 2017). Then, 4 weeks after the start of vGCV protocol, GFAP-Tk+ animals and their littermates were submitted to the CORT protocol (35 μg/mL), in presence or absence of fluoxetine (18 mg/kg/ day in the drinking water) for the last 4 weeks of the protocol.

2.4.4 | Lipopolysaccharide study

A week after receiving 5-Bromo-2-Deoxyuridine (BrdU), C57BL/6JRj mice were anesthetized with chloral hydrate (400 mg/kg, i.p.). Lipopolysaccharide from *Escherichia coli* O111:B4 (LPS, Sigma-Aldrich; 1 μg) was infused at a flow rate of 0.25 μL/min during 2 min (LEGATO™ 180 syringe pump, KD Scientific Inc.) in the dorsal DG (stereotaxic coordinates in mm from bregma: $A = -1.4$, $L = \pm 1.0$, $V = -1.75$; A, anterior; L, lateral; and V, ventral; Chugh et al., 2013). Animals were killed 24 h, 3, or 7 days after LPS injection for immunochemistry.

FIGURE 1 β-arrestin-2 expression is involved in chronic fluoxetine-induced anxiolytic/antidepressant-like effects. (a) Experimental protocol timeline to assess behavioral and neurogenic consequences of a 4-week fluoxetine treatment (18 mg/kg/day in the drinking water) in β-arrestin-2 Heterozygous (β-Arr2 Hets), knockout mice (β-Arr2 KO) mice compared with their wild-type (WT) littermates. (b-h) To evaluate the survival of newborn cells, 5-Bromo-2-Deoxyuridine (BrdU) was administered twice daily at 150 mg/kg intraperitoneally, for three consecutive days, 5 weeks before killing. Anxiety was expressed as the time spent in the center (b), the total entries in the center (c), the total ambulatory distance (d) during 30 min in the open field, and as time spent (e) or entries (f) in open arms of the elevated plus maze. In the novelty-suppressed feeding, latency time to feed was measured (g), and food consumption in the home cage (h). Values plots are mean ± SEM ($n = 5$–8 animals/group). Data were analyzed with a two-way ANOVA (see Table S1). Significant main effects and/or interactions were followed by Fisher's PLSD post hoc analysis (see Table S1). $^{*}p < .05$, $^{**}p < .01$ for comparisons between vehicle-treated WT and fluoxetine-treated WT mice; $\#p < .05$, $\#\#p < .01$ for comparisons between fluoxetine-related β-Arr2 Hets or β-Arr2 KO and vehicle-treated WT mice; §§$p < .01$ for comparisons between fluoxetine-treated β-Arr2 Hets or β-Arr2 KO and fluoxetine-treated WT mice.

10981063, 2023, 10, Downloaded from https://onlinelibrary.wiley.com/doi/10.1002/hipo.23568 by Université de Versailles-Saint-Quentin-en-Yvelines, Wiley Online Library on [15/11/2023]. See the Terms and Conditions (https://onlinelibrary.wiley.com/terms-and-conditions) on Wiley Online Library for rules of use; OA articles are governed by the applicable Creative Commons License

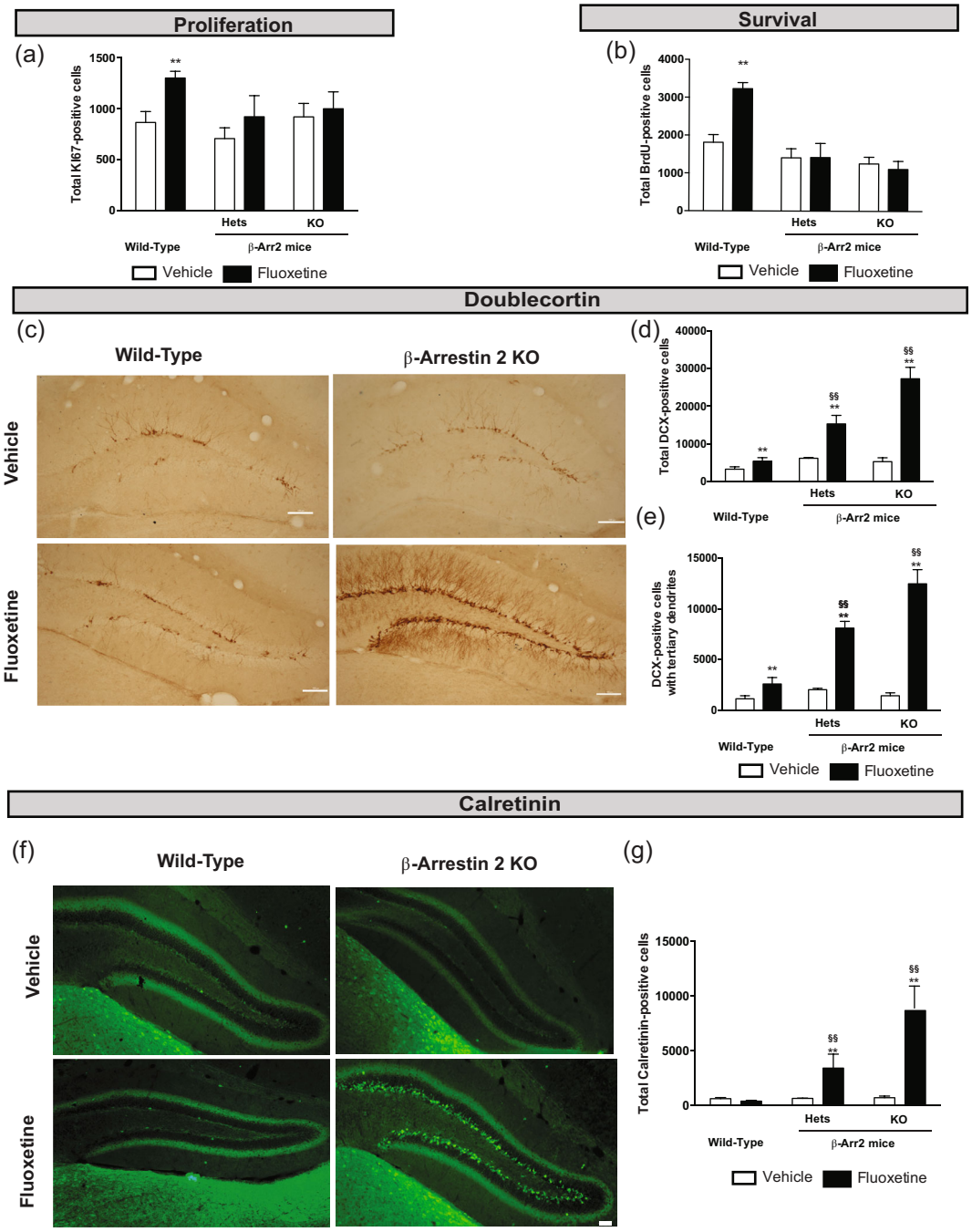

FIGURE 2 β-arrestin-2 expression is required for chronic fluoxetine treatment, increasing the survival of newborn cells but not maturation of young neurons. (a–g) The effects of 28 days of treatment with fluoxetine (18 mg/kg/day) on cell proliferation (a), cell survival (b), and maturation of young neurons (c–g) were compared to those of vehicle in β-arrestin-2 Heterozygous (β-Arr2 Hets), knockout mice (β-Arr2 KO) mice compared with their wild-type (WT) littermates. Proliferation (a) and survival (b) are measured as Ki67+ and BrdU+ cells, respectively. Maturation was characterized by the total number of DCX+ cells (d), the number of DCX+ cells with tertiary dendrites (e), and calretinin+ cells (g). Images of doublecortin or calretinin staining following vehicle or fluoxetine treatment in β-Arr2 KO mice and their WT littermates (10× magnification, scale bar = 100 μm) (c, f). Values plot are mean ± SEM (n = 3/4 animals/group). Data were analyzed with a two-way ANOVA (see Table S2). Significant main effects and/or interactions were followed by Fisher's PLSD post hoc analysis (see Table S2). *p < .05; **p < .01 for comparisons between vehicle-treated and fluoxetine-treated groups for each genotype; §§p < .01 for comparisons between fluoxetine-treated β-Arr2 Hets or β-Arr2 KO and fluoxetine-treated WT mice.

10981063, 2023, 10, Downloaded from https://onlinelibrary.wiley.com/doi/10.1002/hipo.23568 by Université de Versailles-Saint-Quentin-en-Yvelines, Wiley Online Library on [15/11/2023]. See the Terms and Conditions (https://onlinelibrary.wiley.com/terms-and-conditions) on Wiley Online Library for rules of use; OA articles are governed by the applicable Creative Commons License

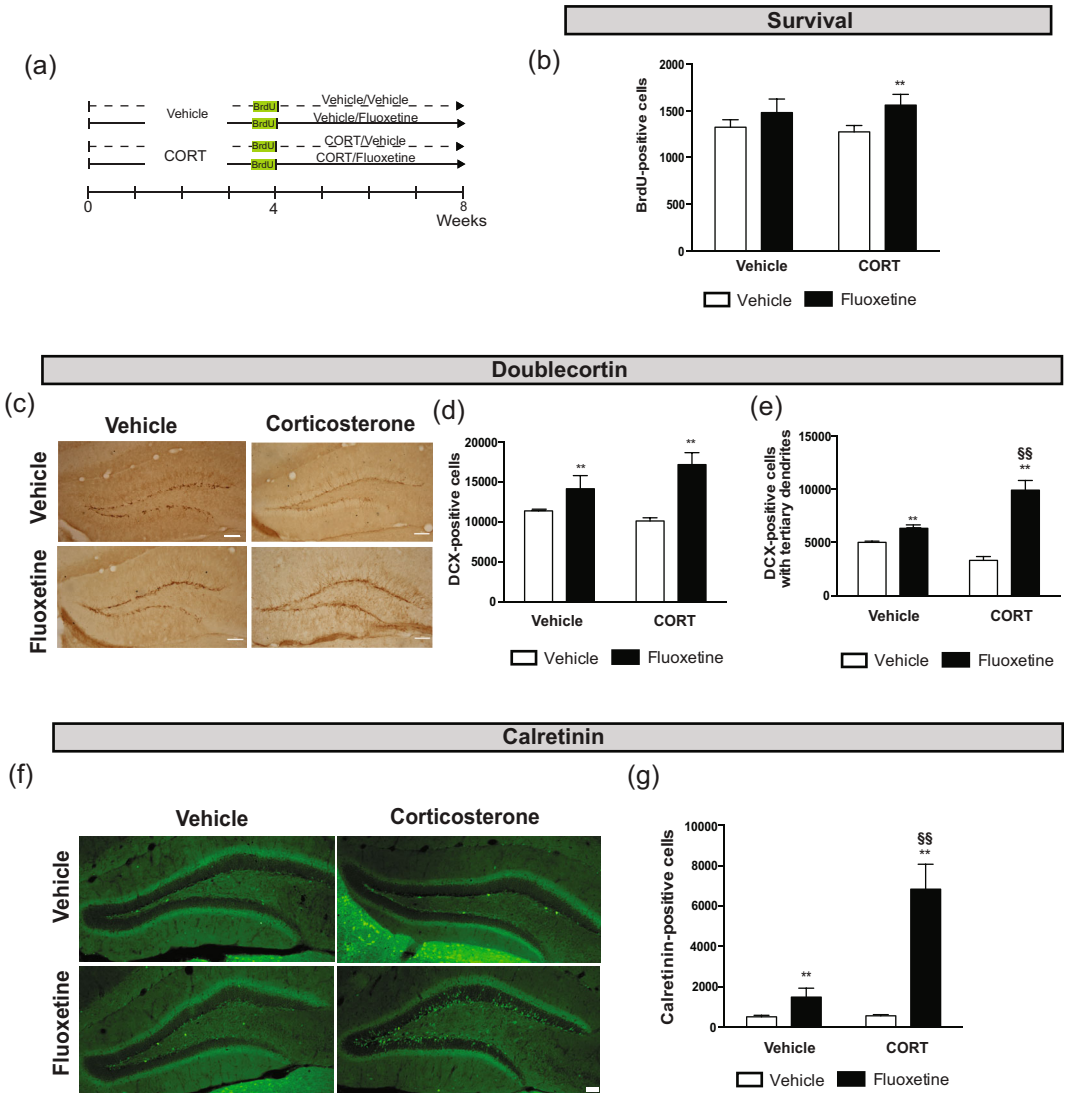

FIGURE 3 Chronic fluoxetine treatment increased doublecortin and calretinin expression in adult dentate gyrus independently from adult hippocampal neurogenesis. (a) Experimental protocol timeline to assess survival and dendritic maturation of young neurons in the DG of the hippocampus of 8 weeks of corticosterone (35 μg/mL in the drinking water) ± fluoxetine (18 mg/kg/day in the drinking water) during the last 4 weeks. To evaluate the survival of newborn cells, 5-Bromo-2-Deoxyuridine (BrdU) was administered twice a day at 150 mg/kg, intraperitoneally, for 3 days and 4 weeks before killing. (b–g) The effects of 28 days of treatment with fluoxetine (18 mg/kg/day) on cell survival (b) and maturation of young neurons (c–g) were compared to those of vehicle in corticosterone-treated mice or not. Survival (B) was measured BrdU+ cells. Maturation was characterized by the total number of DCX+ cells (d), the number of DCX+ cells with tertiary dendrites (e), and calretinin+ cells (g). Images of doublecortin or calretinin staining following vehicle or fluoxetine treatment in corticosterone-treated animals or not. 10× magnification (scale bar = 100 μm) (c, f). Values plots are mean ± SEM ($n = 3–5$ animals/group). Data were analyzed with a two-way ANOVA (see Table S6). Significant main effects and/or interactions were followed by Fisher's PLSD post hoc analysis. $^{**}p < .01$ for comparisons between fluoxetine-treated and vehicle-treated groups in control (vehicle) or CORT mice; §§$p < .01$ comparisons between fluoxetine-treated CORT and fluoxetine-treated control groups.

2.5 | Behavioral study in β-Arr2 −/− KO mice

The same cohort of animals was tested in three different behavioral models of anxiety and depression. Each animal, over a week, was successively tested in the open field (OF), elevated plus maze (EPM), and novelty-suppressed feeding (NSF). Behavioral testing occurred during the light phase between 0700 and 1900. Behavioral paradigms occurred after 28 days of fluoxetine treatment (Figure 1).

2.5.1 | Open field

This test was performed as described by Faye et al. (2019). Motor activity was quantified in four 39 × 39 cm^2 Perspex plastic OF boxes (Vivo-tech/Ugo Basile). The apparatus was illuminated from the ground with special designed 40 × 40 cm^2 infrared backlights (monochromatic wavelength 850 nm high homogeneity, Vivo-tech). Activity chambers were monitored by four black and white cameras with

10981063, 2023, 10, Downloaded from https://onlinelibrary.wiley.com/doi/10.1002/hipo.23568 by Université de Versailles-Saint-Quentin-en-Yvelines, Wiley Online Library on [15/11/2023]. See the Terms and Conditions (https://onlinelibrary.wiley.com/terms-and-conditions) on Wiley Online Library for rules of use; OA articles are governed by the applicable Creative Commons License

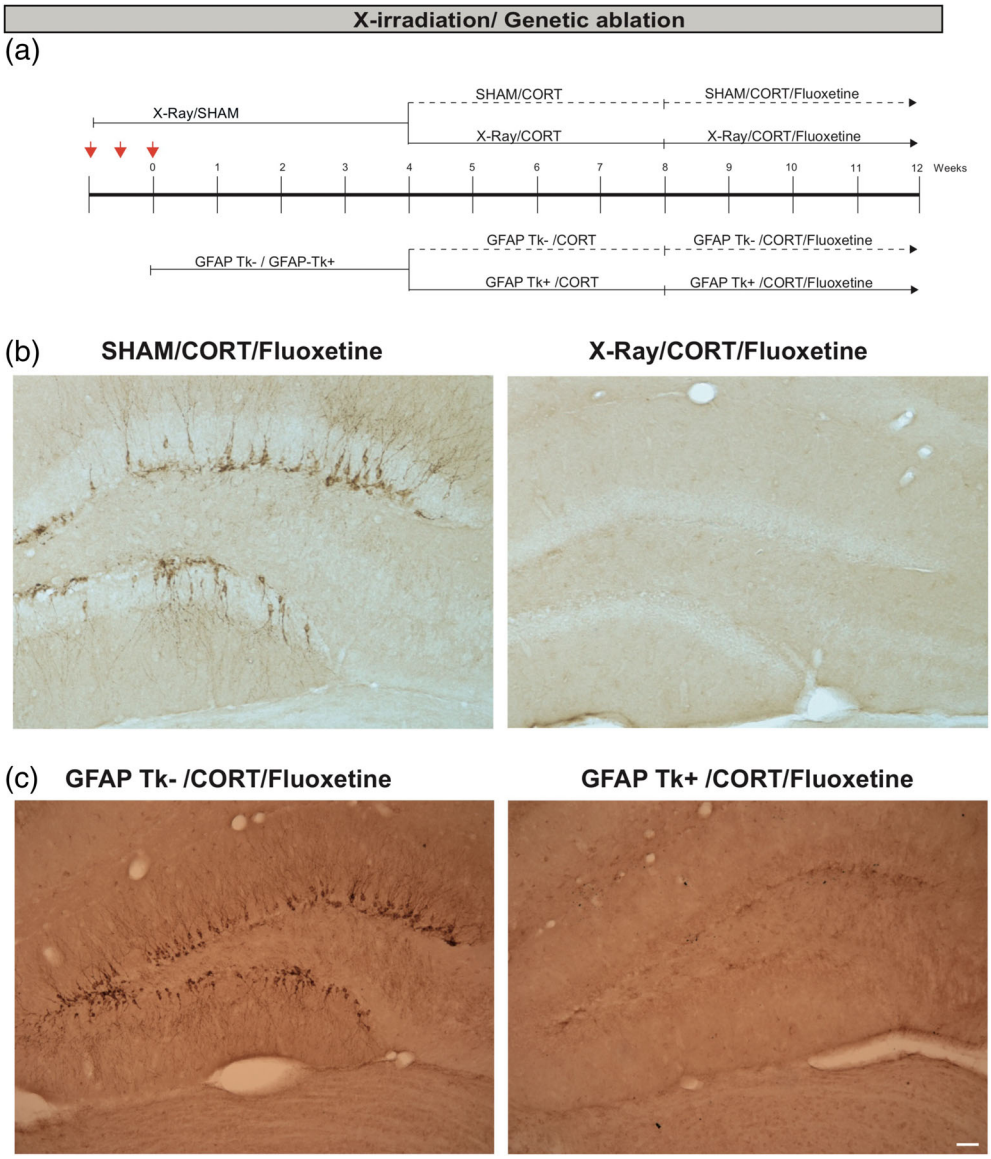

FIGURE 4 Doublecortin expression is sensitive to adult hippocampal neurogenesis ablation. (a) Experimental protocol timeline to assess consequences of arresting adult hippocampal neurogenesis using focal X-irradiation or pharmacogenetic in chronic fluoxetine-treated mice (18 mg/kg/day for 28 days in the drinking water) in a stress-related model of Anxiety/Depression after 4 weeks of corticosterone (35 μg/mL in the drinking water). X-irradiation occurred a month before the start of corticosterone treatment to ensure that markers of inflammation were indistinguishable from sham animals. Genetic ablation was performed using GFAP TK+ mice receiving vGCV a month before the start of corticosterone. (b) Images of doublecortin staining following chronic fluoxetine treatment in X-irradiated or sham corticosterone-treated animals (10× magnification). (c) Images of doublecortin staining following chronic fluoxetine treatment in GFAP-TK+ or GFAP-TK- mice under corticosterone treatment (10× magnification, scale bar = 100 μm).

varifocal optics and polarizing filters (Vivo-tech). The whole setup was controlled using ANYMAZE version 6 video tracking software (Stoelting Co/Vivo-tech). Dependent measures were time in the center over 30 min for systemic administration or 6-min test period for optogenetic experiments, total ambulatory distance, and ambulatory distance traveled in the center divided by total distance.

2.5.2 | Elevated plus maze

This test was performed as described by Faye et al. (2019). The maze is a plus-cross-shaped apparatus, with two open arms and two arms closed by walls linked by a central platform 50 cm above the floor. Mice were individually put in the center of the maze facing an open arm and were allowed to explore the maze for 5 min. The time spent in and the number of entries into the open arms were used as an anxiety index. All parameters were measured using a videotracker (EPM3C, Bioseb).

2.5.3 | Novelty-suppressed feeding

The NSF is a conflict test that elicits competing motivations: the drive to eat and the fear of venturing into the center of a brightly lit arena. The latency to begin eating is used as an index of anxiety/depression-like behavior, because classical anxiolytic drugs and chronic antidepressants decrease this measure (David et al., 2009). The NSF test was carried out during a 15-min period, as previously described. Briefly, the testing apparatus consisted of a plastic box (50 × 50 × 20 cm), the floor of which was covered with approximately 2 cm of wooden bedding. Twenty-four hours before behavioral testing, all food was removed from the home cage. At the time of testing, a single pellet of food (regular chow) was placed on a white paper platform positioned in the center of the box. Each animal was placed in a corner of the box, and a stopwatch was immediately started. The latency to eat (defined as the mouse sitting on its haunches and biting the pellet using forepaws) was timed.

10981063, 2023, 10, Downloaded from https://onlinelibrary.wiley.com/doi/10.1002/hipo.23568 by Université de Versailles-Saint-Quentin-en-Yvelines, Wiley Online Library on [15/11/2023]. See the Terms and Conditions (https://onlinelibrary.wiley.com/terms-and-conditions) on Wiley Online Library for rules of use; OA articles are governed by the applicable Creative Commons License

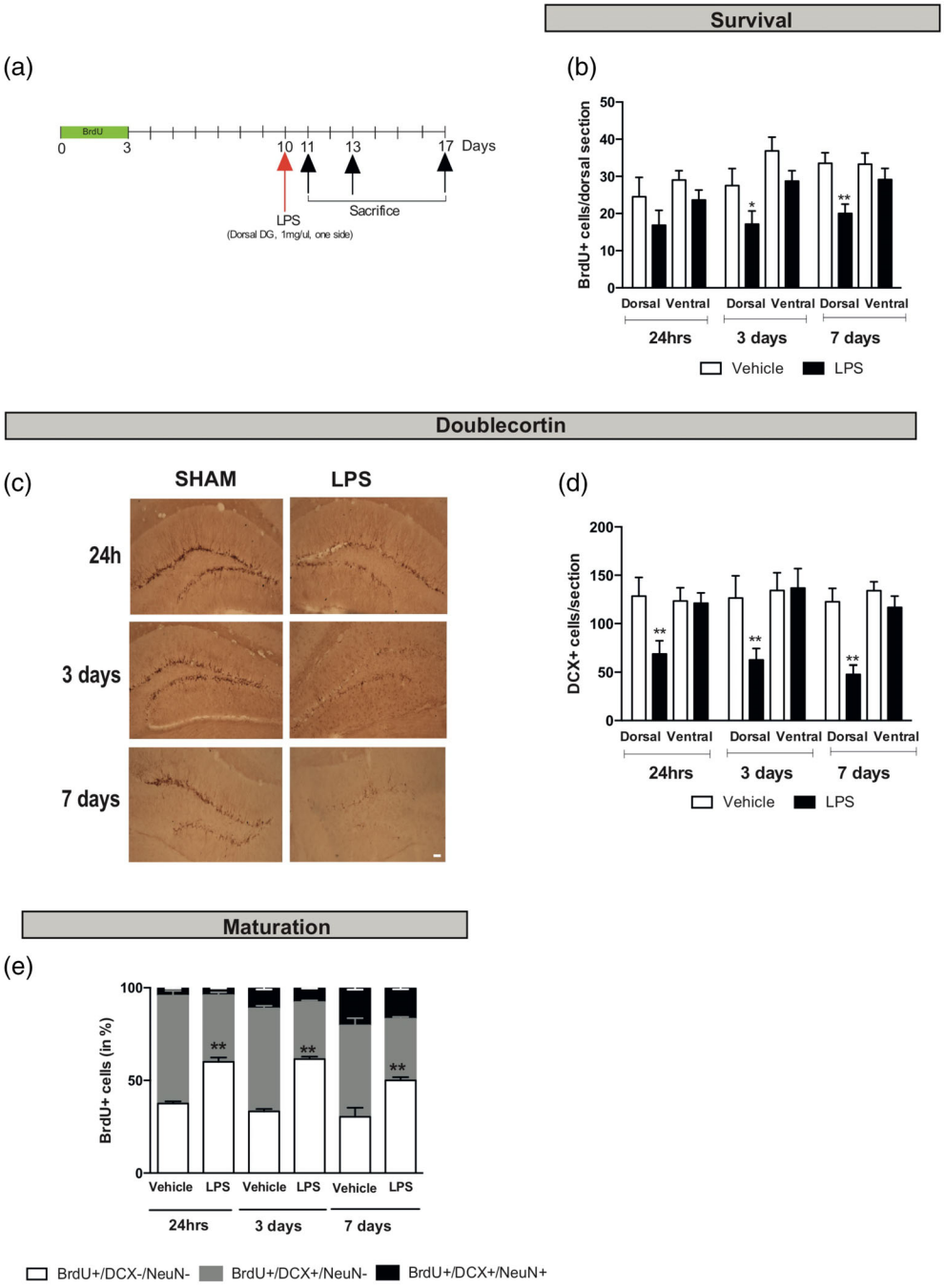

FIGURE 5 Injecting a pro-inflammatory lipopolysaccharide in the mouse dorsal dentate gyrus, induced a large reduction in doublecortin expression. (a) Experimental protocol timeline to assess consequences of a unilateral lipopolysaccharide (LPS) infusion (1 mg/μL) in the dorsal DG on survival and dendritic maturation of young neurons. To evaluate the survival of newborn cells, 5-Bromo-2-Deoxyuridine (BrdU) was administered twice a day at 150 mg/kg intraperitoneally for 3 days, 7, 10, or 14 days before killing. (b–e) The effects of LPS-induced inflammation on survival of newborn cells (b), DCX+ cells (c, d), or maturation of newborn neurons were quantified by the number of Brdu+ cells in the dorsal DG at the injected side (right side, R) and compare to the control-lateral side (left side, R) 24 h, 3- and 7-day post-injection along the dorso/lateral axis (e). Images of doublecortin staining (c) following LPS infusion at 24 h, 3, and 7 days compared to the vehicle-injected side (10× magnification, scale bar = 100 μm). The effect of LPS on DCX+ cells was measured at the injected (R) along the dorso-lateral axis, 24 h, 3-, and 7 day post-injection when compared and the control-lateral vehicle-injected side (L) (d). The fate of surviving BrdU+ was investigated by triple staining using co-localization of BrdU+ cells with markers of neuronal maturation (DCX) and mature neurons (NeuN) 24 h, 3-, and 7-day post-LPS injection (f). Values plot are mean ± SEM ($n = 3–7$ animals/group). Data were analyzed with a one-way ANOVA with repeated measures (see Table S9). Significant main effects and/or interactions were followed by Fisher's PLSD post hoc analysis (see Table S4). *$p < .05$; **$p < .01$ for comparisons between the LPS-injected and the vehicle-injected side along the dorsal/ventral axis.

10981063, 2023, 10, Downloaded from https://onlinelibrary.wiley.com/doi/10.1002/hipo.23568 by Université de Versailles-Saint-Quentin-en-Yvelines, Wiley Online Library on [15/11/2023]. See the Terms and Conditions (https://onlinelibrary.wiley.com/terms-and-conditions) on Wiley Online Library for rules of use; OA articles are governed by the applicable Creative Commons License

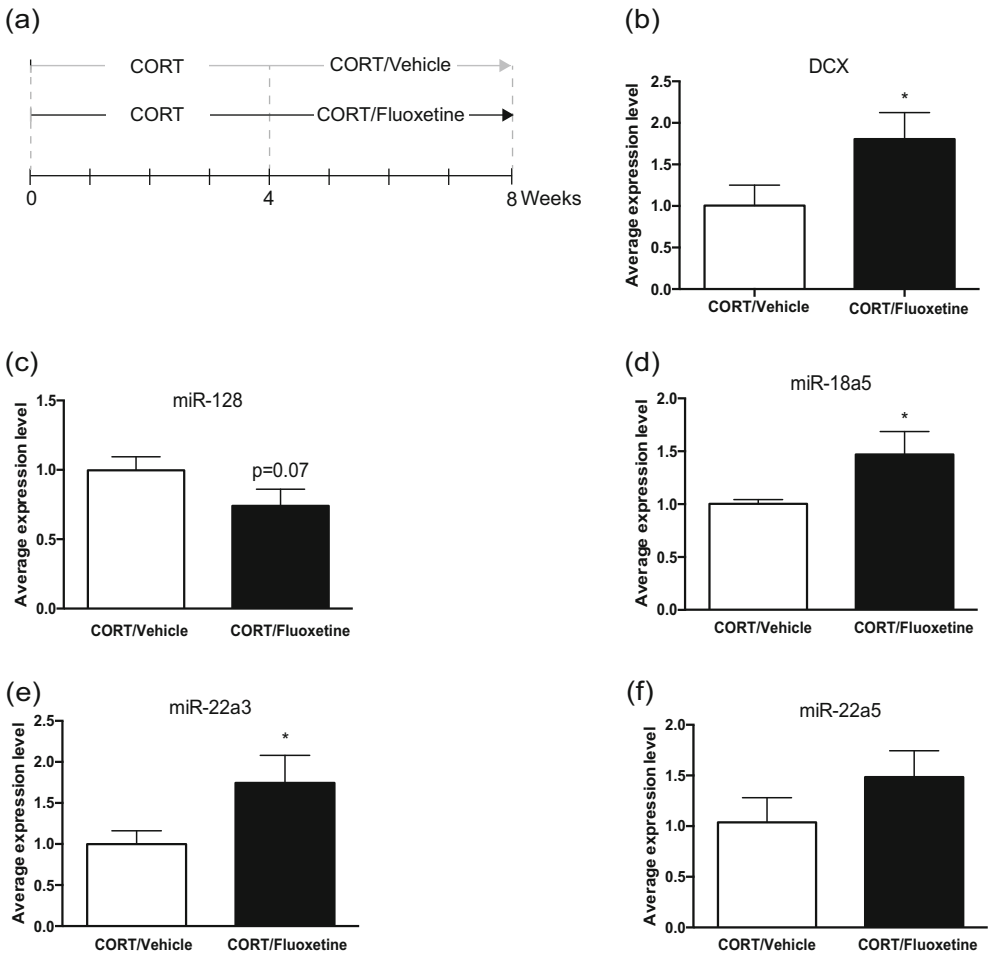

FIGURES 6 Chronic fluoxetine increased hippocampal doublecortin expression in a stress-related model of Anxiety/Depression modulates the expression of microRNA. (a) Experimental protocol timeline to assess the effect of chronic fluoxetine treatment (18 mg/kg/day in the drinking water) in a stress-related model of Anxiety/Depression after 4 weeks of corticosterone (CORT, 35 μg/mL in the drinking water) on hippocampal DCX and microRNA (miR) expression. (b–f) Values plot are mean ± SEM ($n = 4–5$ animals/group). Data were analyzed with an unpaired *t*-test (see Table S10). $^*p < .05$ unpaired *t-tests* between CORT/fluoxetine and CORT/vehicle-treated groups.

Immediately afterward, the animal was transferred to its home cage, and the amount of food consumed by the mouse in the subsequent 5 min was measured, serving as a control for change in appetite as a possible confounding factor.

2.6 | Immunohistochemistry

The effects of chronic treatment with fluoxetine on AHN (proliferation and/or survival and/or maturation) were assessed in β-Arr1 KO, β-Arr2 Hets, β-Arr2 KO mice, and their WT littermates, in the CORT-treated mice presenting an intact or ablation of AHN or infusion of LPS in the dorsal DG.

Thus, at the end of each procedure, animals were anesthetized with ketamine and xylazine (100 mg/mL ketamine; 20 mg/mL xylazine), and then perfused transcardially (cold saline for 2 min, followed by 4% cold para-formaldehyde at 4°C). The brains were then removed and cryoprotected in 30% sucrose and stored at 4°C. Serial sections (35 μm) were cryosectioned through the entire hippocampus (−1.10 to −3.80 mm) relative to Bregma according to Franklin and Paxino's brain atlas (Franklin & Paxinos, 2007) stored in phosphate-buffered saline (PBS) with 0.1% NaN_3.

Since LPS was only injected in the dorsal DG, its consequences, the contralateral side and along the septotemporal axis of the DG were also analyzed. The coordinates used to dissociate the dorsal and ventral hippocampus were based on previous publications (Rainer et al., 2012): from −1.10 to −2.50 mm relative to Bregma for the dorsal hippocampus and from −2.50 to −3.80 mm for the ventral hippocampus according to Franklin and Paxino's brain atlas (Franklin & Paxinos, 2007).

2.6.1 | Proliferation study

For Ki67 immunostaining, sections were incubated in 0.3% triton in PBS and 10% normal donkey serum (NDS). Then sections were incubated overnight at 4°C with anti-rabbit Ki67 (from Vector; 1:100). After washing with PBS, sections were incubated for 2 h with secondary antibody (1:200 biotinylated donkey anti-rabbit) followed by amplification with an avidin–biotin complex. The staining was visualized with DAB. Ki67 cells were counted using a BX51 microscope (Olympus) in the DG at ×20 magnificence. An unbiased and blinded protocol was used to count the KI67-labeled cells in the granule cell layer (GCL) of the DG along its septotemporal axis. For quantification,

10981063, 2023, 10, Downloaded from https://onlinelibrary.wiley.com/doi/10.1002/hipo.23568 by Université de Versailles-Saint-Quentin-en-Yvelines, Wiley Online Library on [15/11/2023]. See the Terms and Conditions (https://onlinelibrary.wiley.com/terms-and-conditions) on Wiley Online Library for rules of use; OA articles are governed by the applicable Creative Commons License

12 matched sections were selected for each mouse from bregma −1.10 to −3.80 mm.

2.6.2 | Survival study

Mice were administered with 5-Bromo-2-Deoxyuridine (BrdU) (150 mg/kg, twice daily for three consecutive days) before the initiation of the various treatments as described by Mendez-David et al. (2014). For DAB staining, sections were mounted on slides, boiled in citric acid (pH 6.0) for 5 min, rinsed with PBS, and treated with 0.01% trypsin in Tris/$CaCl_2$ for 10 min. Brain sections were incubated for 30 min with 2 N HCl and blocked with 5% NGS. Sections were then incubated overnight at room temperature with anti-mouse BrdU (1:100). After washing with PBS, sections were incubated for 1 h with secondary antibody (1:200 biotinylated goat anti-mouse) followed by amplification with an avidin–biotin complex. The BrdU staining was visualized with DAB at ×20 magnificence using a BX51 microscope (Olympus). An unbiased and blinded protocol was used to count the BrdU-labeled cells in the GCL of the DG along its septotemporal axis. For quantification, 12 matched sections were selected for each mouse from bregma −1.10 to −3.80 mm.

2.6.3 | DCX labeling

The immunohistochemistry protocol was adapted from David et al. (2009). Sections were rinsed in PBS, treated with 1% H_2O2 in 1:1 PBS and methanol for 15 min to quench endogenous peroxidase activity (and to enhance dendritic staining), incubated in 10% NDS and 0.3% Triton X-100 for 30 min, and then incubated overnight at 4°C in primary antibody for doublecortin (goat; 1:500; Santa Cruz Biotechnology). The secondary antibody was biotinylated donkey anti-goat (1:500; Jackson ImmunoResearch) in PBS for 2 h at room temperature. Sections were developed using avidin–biotin complex (Vector) and DAB kit. DCX-positive (DCX+) cells were subcategorized according to their dendritic morphology: DCX+ cells with no tertiary dendritic processes and DCX+ cells with tertiary (or higher order) dendrites. The DCX+ staining was visualized with DAB at ×20 magnificence using a BX51 microscope (Olympus). An unbiased and blinded protocol was used to count the DCX-labeled cells in the GCL of the DG along its septotemporal axis. For quantification, six matched sections were selected for each mouse from bregma −1.10 to −3.80 mm.

2.6.4 | Calretinin labeling

For calretinin (CR) immunostaining, sections were incubated in 0.3% Triton in PBS and 10% NDS. Then sections were incubated overnight at 4°C with anti-rabbit CR polyclonal antibody (from Swant; 1:10,000). After washing with PBS, sections were incubated for 2 h with secondary antibody (1:500 Jackson ImmunoResearch). The CR staining was visualized at ×20 magnificence using a BX51 microscope (Olympus). An unbiased and blinded protocol was used to count the DCX-labeled cells in the GCL of the DG along its septotemporal axis. For quantification, six matched sections were selected for each mouse from bregma −1.10 to −3.80 mm.

2.6.5 | Immunohistochemistry and confocal imaging for maturation study

Immunohistochemistry was performed in the following steps: 2 h incubation in 1:1 formamide/2× SSC at 65°C, 5 min rinse in 2× SSC, 30 min incubation in 2 N HCl at 37°C, and 10 min rinse in 0.1 M boric acid, pH 8.5, 2 h incubation in 0.1 M PBS with 0.3% Triton X-100, and 5% NDS. Then sections were incubated overnight at 4°C in primary antibodies for doublecortin (goat 1:500; Santa Cruz Biotechnology), bromodeoxyuridine (BrdU; rat; 1:100; Serotec), and neuronal-specific nuclear protein (NeuN; mouse; 1:500; Chemicon). Then fluorescent secondary antibodies were used. All secondary antibodies were purchased from Jackson ImmunoResearch (1:500). Approximately six sections per animal and 20–30 BrdU+ cells per treatment group were analyzed ($n = 4$–5 animals per condition). To identify co-localization of BrdU+/DCX+/NeuN+, *z*-stacks of immunolabeled sections were obtained using a confocal scanning microscope (Leica TCS SP8, Leica Microsystems Inc.) equipped with three simultaneous PMT detectors.

2.7 | Hippocampal doublecortin and microRNA expression

2.7.1 | Hippocampal microdissection and preparation of total RNA

Mouse hippocampal tissues were isolated and frozen in liquid nitrogen, and tissue was stored at −80°C. Total RNA was isolated from frozen tissue samples using TRIzol (Invitrogen) and according to the manufacturer's protocol. RNA quality was assessed using a BioMate™ 3S spectrophotometer (Thermo Fisher Scientific). RNA quality was assessed using the Biophotometer (Eppendorf) and gel electrophoresis with the RNA LabChip® 6000 Nano kit (Bioanalyzer® 2000, Agilent Technologies). RNA integrity was evaluated by capillary electrophoresis using RNA 6000 Nanochips and the Bioanalyzer 2100 (Agilent Technologies). All RIN score values were above 8.0.

2.7.2 | RT-qPCR analysis

For quantification of mRNA or miRNA expression, first-strand cDNA was synthesized from 0.2 to 1 μg of total RNA, using the miSCRIPT® II RT kit (Qiagen), according to the manufacturer's instructions. PCR forward primer specific to each target gene was designed from the RefSeq sequence using Primer3Plus software (https://primer3plus.com/cgi-bin/dev/primer3plus.cgi). The cDNA synthesized from 3 ng

10981063, 2023, 10, Downloaded from https://onlinelibrary.wiley.com/doi/10.1002/hipo.23568 by Université de Versailles-Saint-Quentin-en-Yvelines, Wiley Online Library on [15/11/2023]. See the Terms and Conditions (https://onlinelibrary.wiley.com/terms-and-conditions) on Wiley Online Library for rules of use; OA articles are governed by the applicable Creative Commons License

TABLE 2 Oligonucleotide sequences for quantification of mRNA or miRNA expression.

Oligonucleotides			
mmu-miR-22-3p	GCTGCCAGTTGAAGAACTG	Integrated DNA Technologies (IDT)	Custom single-stranded DNA oligo (25 nmol)
mmu-miR-22-5p	AGTTCTTCAGTGGCAAGCTT	IDT	Custom single-stranded DNA oligo (25 nmol)
mmu-miR-29a-3p	GCACCATCTGAAATCGG	IDT	Custom single-stranded DNA oligo (25 nmol)
mmu-miR-29a-5p	ACTGATTTCTTTTGGTGTTCAG	IDT	Custom single-stranded DNA oligo (25 nmol)
mmu-miR-34a-3p	AATCAGCAAGTATACTGCCCT	IDT	Custom single-stranded DNA oligo (25 nmol)
mmu-miR-34a-5p	TGGCAGTGTCTTAGCTGG	IDT	Custom single-stranded DNA oligo (25 nmol)
mmu-miR-124-3p	CACGCGGTGAATGCC	IDT	Custom single-stranded DNA oligo (25 nmol)
mmu-miR-18a-5p	TAAGGTGCATCTAGTGCAGATAG	IDT	Custom single-stranded DNA oligo (25 nmol)
mmu-miR-19a-3p	GTGCAAATCTATGCAAAACTG	IDT	Custom single-stranded DNA oligo (25 nmol)
Rnu6	CGCAAGGATGACACGCAAATTC	IDT	Custom single-stranded DNA oligo (25 nmol)
Snord87	TAAGTTTTTGCCGTTTACCC	IDT	Custom single-stranded DNA oligo (25 nmol)
Snord62	TGCTAAAAGAGTGGCAAGG	IDT	Custom single-stranded DNA oligo (25 nmol)
Snord68	TTGATGAAAGTACTTTTGAACCC	IDT	Custom single-stranded DNA oligo (25 nmol)
miR128_Mm1_F	TCACAGTGAACCGGTCTC	IDT	Custom single-stranded DNA oligo (25 nmol)
miR142_Mm1_F	TGTAGTGTTTCCTACTTTATGGA	IDT	Custom single-stranded DNA oligo (25 nmol)

of total RNA was amplified in a CFX384™ real-time thermal cycler (Bio-Rad), either for miR quantitation using the miSCRIPT SYBR® Green PCR kit (Qiagen) according to the manufacturer's instructions, with final concentrations of 500-nM forward primer and 1× reverse universal primer, in triplicate 10-µL reactions, by 40 cycles (94°C 10 s; 56°C 25 s; and 70°C 20 s), or for mRNA quantitation using the Sso Advanced SYBR® Green PCR kit (Bio-Rad) according to the manufacturer's instructions, with 500-nM final concentrations of each primer (Table 2), in triplicate 10-µL reactions, by 45 two-step cycles (94°C 10 s and 60°C 25 s). "No RT" controls were amplified to check for the absence of genomic DNA contamination, and melting curve analysis was performed to assess the purity of the PCR products. PCR efficiencies calculated for each gene from the slopes of calibration curves generated from the pool of all cDNA samples were above 95%. Gapdh and Actb genes were used as references for normalization of mRNA expression results, and Rnu6, Snora62, Snord68, and Snord87 for miR expression results. The normalized relative expression of target genes in samples was determined using the $^{\Delta\Delta}$Cq method with correction for PCR efficiencies, where $NRQ = E_{Target}{}^{-\Delta Cq\ Target}/E_{Ref}{}^{-\Delta Cq\ Reference}$ and $^{\Delta}Cq = Cq_{sample} - Cq_{calibrator}$ (Hellemans et al., 2007). Final results were expressed as the *n*-fold differences in target gene expression in treated versus vehicle cells. Mean values ± SEM from both mice groups are presented.

2.8 | Statistical analysis

Results from data analyses, expressed as mean ± SEM were analyzed using Prism 8.3 software (GraphPad). For all experiments, unpaired *t* test, one-way analysis of variance (ANOVA) with repeated measures, or two-way ANOVAs were applied to the data as appropriate. Significant main effects and/or interactions were followed by Fisher's PLSD post hoc analysis. Statistical significance was set at $p < .05$. All statistical tests and *p* values are listed in Tables S1–S9.

3 | RESULTS

1. **The antidepressant/anxiolytic effects of fluoxetine are absent in the β-Arr2 heterozygote and KO mice.**

We have been investigating the mechanisms underlying the antidepressant/anxiolytic effects of fluoxetine (18 mg/kg/day) in a variety of animal models. Our previous studies showed that β-Arr2 was necessary for several of the behavioral effects of chronic fluoxetine (David et al., 2009). Here, we have confirmed these findings by comparing the effects of a 4-week fluoxetine treatment in WT, β-arrestin-2 heterozygote (β-Arr2 Het), and knockout (β-Arr2 KO) mice in three anxiety/depression tests: the OF, the EPM, and the NSF test (Figure 1a). A two-way ANOVA on all anxiety-related parameters revealed that chronic fluoxetine treatment had an effect in WT in the three paradigms (Table S1), resulting in an increase in time spent (Figure 1b) and total entries in the center in the OF (Figure 1c) without affecting locomotor activity (Figure 1d), increase in time spent (Figure 1e) and a trend for entries (Figure 1f) in open arms in the EPM, a trend for a decrease in latency to feed in the NSF (Figure 1g) without affecting food consumption (Figure 1h). All these fluoxetine-induced anxiolytic/antidepressant effects are absent in β-Arr2 KO mice (Figure 1b–e). Interestingly, these anxiolytic/antidepressant effects of fluoxetine are also absent in the β-Arr2 Het mice, which indicates that both alleles of β-Arr2 are necessary for the effects of fluoxetine. In keeping with our previous findings (David et al., 2009), the β-Arr2 KO display more anxiety-related behaviors than their WT littermates as shown by a decrease in time spent in the center and

10981063, 2023, 10, Downloaded from https://onlinelibrary.wiley.com/doi/10.1002/hipo.23568 by Université de Versailles-Saint-Quentin-en-Yvelines, Wiley Online Library on [15/11/2023]. See the Terms and Conditions (https://onlinelibrary.wiley.com/terms-and-conditions) on Wiley Online Library for rules of use; OA articles are governed by the applicable Creative Commons License

entries in the center of the OF, a trend for a decrease in time spent in the open arms of the EPM and an increase in latency to feed in the NSF (Figure 1b–e). In addition, we show here that the β-Arr2 Het mice display an intermediate phenotype between the WT and the KOs in most anxiety-related values (Figure 1b–e).

2. **The effects of fluoxetine on neurogenesis are absent in the β-Arr2 heterozygous and KO mice but paradoxically, the expression of two markers of immature neurons, doublecortin and calretinin, is dramatically upregulated by fluoxetine in KO mice.**

Since AHN has been implicated in some of the effects of antidepressants (David et al., 2009; Lino de Oliveira et al., 2020; Santarelli et al., 2003), we also examined the effects of chronic fluoxetine treatment on various stages of the neurogenesis process in the β-Arr2 Het and β-Arr2 KO mice. Proliferation in the SGZ was assessed by the level of KI67, a marker of dividing cells; survival of the young neurons was assessed by retention of the BrdU nucleotide analog injected 5 weeks before sacrif; and numbers of immature neurons were assessed by immunocytochemistry against two markers of immature neurons: DCX and CR which are expressed during the first month of the maturation of young adult-born neurons (Kempermann et al., 2015).

A two-way ANOVA revealed that the stimulatory effect of fluoxetine on proliferation and survival observed in WT mice (Figure 2a,b) was absent in β-Arr2 Het and KO mice (Table S2). These results mirror the behavioral effects of fluoxetine and suggest that the anxiolytic/antidepressant-like effects of fluoxetine may be mediated at least in part by an increase in neurogenesis.

Surprisingly, the effects of fluoxetine on the expression of two markers of immature neurons, DCX and CR were dramatically different from the effects of fluoxetine on proliferation and survival. A two-way ANOVA revealed a massive upregulation of DCX and CR in the β-Arr2 KO mice (Figure 2c–g) even though these mice do not display any increase in neurogenesis as measured by KI67 and BrdU incorporation (Figure 2a,b). This upregulation of DCX and CR appears to be dependent on the expression level of β-Arr2 because it is intermediate in the β-Arr2 Het mice (Figure 2c–g). A previous study demonstrated that the survival and maturation of adult-generated hippocampal neurons do not require DCX (Dhaliwal et al., 2015). Similarly, we found that the number of DCX-expressing cells in the DG is dissociated from levels of neurogenesis; namely in the β-Arr2 Het and KO mice where neurogenesis is not increased by fluoxetine neither at the level of proliferation in the SGZ nor at the level of survival of the young neurons, DCX and CR expressing cells are massively upregulated. This suggests that the levels of these proteins can be increased without a change in neuronal number and that this upregulation only happens when β-Arr2 levels are decreased.

To better understand the nature of the supernumerary cells expressing DCX, that is, to address the hypothesis of defective exit of immaturity, β-Arr2, and their WT littermates were injected BrdU (150 mg/kg, i.p twice daily for three consecutive days) 1 month before the start of a 4-week fluoxetine treatment (18 mg/kg/day drinking water; Figure S1, Table S3). A two-way ANOVA revealed a significant increase in the percentage of BrdU+/DCX+ cells in β-Arr2 KO in comparison to their WT littermates. As expected, the number of double-labeled cells is very low in the control mice because most young neurons older than 4 weeks no longer express DCX (Kempermann et al., 2003). The increased number of double-labeled cells in the β-Arr2 KO could be explained by a longer period for the DCX+ cells to become mature neurons or the fact that some of them stay in an immature state.

Since there are multiple examples of nonproliferative neuronal precursors residing outside the neurogenic niches (Benedetti et al., 2020; Benedetti & Couillard-Despres, 2022; Bonfanti & Nacher, 2012; Bonfanti & Seki, 2021; Coviello et al., 2021; Feliciano et al., 2015; Gomez-Climent et al., 2011; Klempin et al., 2011; Palazzo et al., 2018; Piumatti et al., 2018; Rotheneichner et al., 2018; Sorrells et al., 2019), we also analyzed the expression of DCX in the piriform cortex of β-Arr2 Het, KO and their littermates (Figure S2, Table S4). We found an increase in total DCX and DCX with tertiary dendrites expression in β-Arr2 KO mice (Figure S2a–c). We also found an elevated basal level of DCX in the β-Arr2 KO compared to the WT. However, no BrdU-positive cells were found (data not shown), confirming previous a report that DCX-expressing cells in the piriform cortex were strictly postmitotic (Klempin et al., 2011). Therefore, this is an instance where DCX can be detected and regulated in a nonneurogenic niche, the piriform cortex (Kremer et al., 2013). Interestingly, in both the hippocampus and pyriform cortex, fluoxetine treatment elicited an increase in DCX levels in the β-Arr2 KO mice.

Since two types of β-arrestins are expressed in the hippocampus (David et al., 2009), β-Arr1 and β-Arr2, we conducted a similar study in the β-Arr1 KO mice (Figure S3, Table S5). Like in the β-Arr2 KO, proliferation and survival were not increased by chronic fluoxetine in the β-Arr1 KO (Figure S3a–c). In contrast, DCX was increased to the same extent in β-Arr1 KO as in the WT (Figure S3d–f). Therefore, we also see a complex relationship between the expression of DCX and levels of neurogenesis in the β-Arr1 KO but to a lesser extent than in the β-Arr2 KO.

3. **In the corticosterone model of anxiety/depression, fluoxetine induces a larger increase in the expression of DCX and calretinin than in levels of neurogenesis.**

We next decided to assess whether a dissociation between neurogenesis and DCX levels can also be found in other situations than in the β-Arr1 or β-Arr2 KO mice. We chose to look at a model of anxiety/depression, the chronic corticosterone (CORT) model (Figure 3), because a few previous studies had shown surprisingly large effects of fluoxetine on DCX-expressing cells in this model (David et al., 2009; Mendez-David et al., 2014; Robinson et al., 2016). This model consists in administering CORT for 4 weeks in the drinking water, which produces an increase in anxiety, and depression-related measures, that can be reversed by a chronic antidepressant treatment (David et al., 2009; Mendez-David et al., 2014; Mendez-David et al., 2017; Figure 3a). In control animals that did not receive CORT,

10981063, 2023, 10, Downloaded from https://onlinelibrary.wiley.com/doi/10.1002/hipo.23568 by Université de Versailles-Saint-Quentin-en-Yvelines, Wiley Online Library on [15/11/2023]. See the Terms and Conditions (https://onlinelibrary.wiley.com/terms-and-conditions) on Wiley Online Library for rules of use; OA articles are governed by the applicable Creative Commons License

fluoxetine elicited a similar modest increase in survival (+11%), and levels of DCX (+24%) or DCX with tertiary dendrites (+26%; Figure 3b–e, Table S6). In contrast, in CORT-treated animals, the increase in DCX-expressing cells after chronic fluoxetine was significantly larger than the increase in survival (Figure 3c,d). This effect was more pronounced when we counted the number of DCX-positive cells with tertiary dendrites (+199%), which are the most differentiated cells (Figure 3e). When we analyzed another marker of immature neurons, calretinin, the effect of fluoxetine in the CORT group was even more dramatic: 12-fold (567 ± 62 vs. 6834 ± 1234 in CORT/vehicle and CORT/fluoxetine, respectively; Figure 3f,g) while the survival was only increased by 22% (1272 ± 68 vs. 1558 ± 115 in CORT/vehicle and CORT/fluoxetine, respectively).

The transition from immature to mature neuronal markers is characterized by a higher order dendritic branching (tertiary and higher) as well as a partial migration from the SGZ into the GCL in mice (Klempin et al., 2011; Kohler et al., 2011) and in non-human primates (Ngwenya et al., 2015). Therefore, we also examined this migration of DCX-positive cells in the CORT model after chronic fluoxetine by counting the proportion of DCX+ cells within the GCL. Like in the case of tertiary dendrites, we found a large increase in the CORT+ fluoxetine group (Figure S4, Table S7).

In aggregate, these results indicate again a dissociation between levels of neurogenesis and expression of DCX and CR, in this case after a chronic treatment with corticosterone.

4. **The ablation of neurogenesis prevents the effect of fluoxetine on DCX and calretinin expression.**

Earlier reports (Kobayashi et al., 2010; Ohira et al., 2013) and recent reviews from the same group (Hagihara et al., 2019; Ohira et al., 2019) had suggested that fluoxetine induced, in addition to neurogenesis, a dematuration of mature granule cells that would lead to the expression of immature markers such as DCX and Calretinin. We wondered, therefore, whether such a dematuration might contribute to the increase in DCX and CR elicited by fluoxetine in the CORT model. To test that hypothesis, we ablated neurogenesis using two different approaches, one with X-irradiation and another one with a pharmacogenetic strategy prior to assessing the impact of fluoxetine on DCX and CR expression in the CORT paradigm (Figure 4). This pharmacogenetic strategy utilizes the glial fibrillary acidic protein (GFAP) promoter driving the Herpes Simplex Virus Thymidine Kinase (TK) gene. As a result, the dividing GFAP-positive progenitor cells die following treatment with the antiviral drug valganciclovir (vGCV) (Mendez-David et al., 2017; Saxe et al., 2006) (Figure 4c). We found no detectable expression of DCX after X-irradiation or in the GFAP-TK+ mice treated with chronic fluoxetine (Figure 4b–d). These results indicate that mature granule cells which are spared in this ablation model, do not contribute significantly to the observed increase in DCX.

As previously shown (Klempin et al., 2011), we also showed that most DCX+ cells co-expressed calretinin another marker of immature neurons and that X-irradiation suppressed the expression of both DCX and calretinin (Figure S5, Table S8). We conclude therefore that the increase in number of DCX and calretinin-expressing cells observed after fluoxetine in the CORT-treated group comes mostly from immature adult-born neurons rather than from a dematuration of mature granule cells.

5. **Inflammation induces a rapid decrease in the number of DCX-expressing cells.**

We decided also to assess the expression of DCX after inflammation because our preliminary result had indicated that the number of DCX-expressing cells decreased dramatically immediately after X-irradiation even though the number of young neurons was not much affected (Burghardt et al., 2012; Denny et al., 2012). To induce inflammation in a controlled way, we performed intrahippocampal administration of Lipopolysaccharide (LPS). LPS is an endotoxin of Gram-negative bacteria, used extensively for inducing an immune response. Unilateral injection of LPS in the dorsal DG was performed at only the right side of the brain and mice were killed at three different time points after LPS injection: 24 h, 3, and 7 days; therefore, the vehicle-injected side and the ventral pole of the DG can be used as controls (Figure 5a). The number of young neurons as measured by BrdU incorporation is not significantly decreased after 24 h of LPS injection (Figure 5b, Table S9). In contrast, in keeping with our previous x-ray data, there is a significant decrease in the number of DCX-expressing cells 24 h after LPS injection and only on the injected side and not on the ventral pole (Figure 5c,d). These results suggest that like X-irradiation, LPS-induced inflammation results in a decrease in the number of DCX-expressing cells in the absence of a significant change in the number of young adult-born neurons. Three and 7 days after LPS injection, the decrease in the number of DCX-expressing cells remains restricted to the injected side and a decrease in the number of young neurons (BrdU labeled) becomes visible although it is less pronounced than the decrease in the number of DCX-expressing cells (Figure 5b–d). In keeping with these results, the fraction of BrdU-positive cells that are also DCX-positive is larger on the control than on the LPS-injected side at all three time points (Figure 5e).

6. **Fluoxetine modulates the expression of miRs that have been implicated in the number of DCX-expressing cells.**

To begin exploring the mechanism underlying the regulation of DCX and CR expression in response to fluoxetine in the CORT model, we first investigated the level of expression of several microRNAs (miR) that have been implicated in the regulation of DCX mRNA expression (Figure 6a). Second, we showed that levels of DCX mRNA are upregulated by fluoxetine in the CORT model by RT-PCR (Figure 6b). Next, we investigated the levels of miR-128, miR-18a5, miR-22a3, and miR-22a5 by RT-PCR (Figure 6c–f, Table S10). We chose miR128 because it had been shown to downregulate the expression of DCX by directly binding on its 3′UTR region (Evangelisti et al., 2009), and miR-18a, miR-22a3, and miR-22a5 because they belong to a cluster shown to regulate neurogenesis as well as anxiety

10981063, 2023, 10, Downloaded from https://onlinelibrary.wiley.com/doi/10.1002/hipo.23568 by Université de Versailles-Saint-Quentin-en-Yvelines, Wiley Online Library on [15/11/2023]. See the Terms and Conditions (https://onlinelibrary.wiley.com/terms-and-conditions) on Wiley Online Library for rules of use; OA articles are governed by the applicable Creative Commons License

and depression related behaviors (Dwivedi, 2013; Jin et al., 2016). Chronic fluoxetine treatment resulted in a trend for a decrease in miR-128 expression (Figure 6c). In contrast, chronic fluoxetine significantly increased the levels of miR-18a5 and miR-22a3 (Figure 6d,e). In regard to miR-22a5, a trend for an increase was also observed (Figure 6d,e). These results are consistent with the previously described impact of these miRs on the number of DCX-expressing cells and neurogenesis. It is therefore possible that these miRs contribute to the regulation of DCX mRNA expression in our fluoxetine group as well as possibly in our other experimental manipulations such as the β-Arr-2 KO and the LPS-induced inflammation.

4 | DISCUSSION

We will briefly discuss the mechanisms that may be responsible for the complex relation between levels of the DCX protein and levels of neurogenesis we have observed in several models, before enlarging the discussion to the current controversy about levels of neurogenesis in the adult human brain and how our current results may inform that controversy.

4.1 | A complex relation between DCX and neurogenesis

The effects of chronic fluoxetine on both anxiety/depression-related behaviors and on hippocampal neurogenesis have been shown to be mediated by several 5-HT receptors, including the 5-HT_{1A} receptor (Samuels et al., 2016; Santarelli et al., 2003), the 5-HT_4 receptor (Kobayashi et al., 2010; Mendez-David et al., 2014) and possibly the 5-HT_{2B} (Diaz et al., 2012), 5-HT_{1B} (Svenningsson et al., 2006), 5-HT_{2C} (Opal et al., 2014), and 5-HT_{5A} receptors (Sagi et al., 2019). In particular, in the case of the 5-HT_{1A} receptor, we have previously shown that 5-HT_{1A} receptors located in mature granule cells of the DG are critical for the antidepressant/anxiolytic effects of chronic fluoxetine and contribute to the effects of fluoxetine on neurogenesis. There is also evidence that the 5-HT_4 receptor is involved in both the behavioral and neurogenic effects of fluoxetine, but it is not known whether it is the DG 5-HT_4 receptors that contribute to these effects. Both 5-HT_{1A} and 5-HT_4 receptors have been shown to engage the β-arrestin signaling pathway (Bohn & Schmid, 2010; Pytka et al., 2018). It is therefore conceivable that the lack of a behavioral response to fluoxetine in the β-Arr2 KO mice is due to a lack of β-Arr2 in the DG and a subsequent inability of the 5-HT_{1A} and 5-HT_4 receptors to engage β-Arr2 signaling pathways such as the MAPK/ERK signaling. Such impairment may also be related to the absence of the effect of fluoxetine on proliferation and survival in the β-Arr2 KO mice. What is most surprising is that the number of DCX and calretinin-expressing cells, which are both markers of immature neurons, are dramatically upregulated by fluoxetine in the β-Arr2 KO mice. Such an observation may be related to the fact that fluoxetine has been shown to accelerate the maturation of young neurons via a faster transition from the DCX-positive stage to the NeuN-positive stage (Sorrells et al., 2018; J. W. Wang et al., 2008). It is possible that the increased number of DCX-expressing cells in the β-Arr2 KO mice is explained by a delayed maturation of these cells.

To investigate mechanisms that may contribute to the regulation of the number of DCX-expressing cells, we analyzed the expression of a number of miRs that had been implicated in stress or the modulation of neurogenesis (for review; Dwivedi, 2014). We find that a chronic fluoxetine treatment modulates the expression of these miRs in a direction, which is consistent with the upregulation of DCX mRNA expression by fluoxetine. Such results suggest that these miRs may be responsible at least in part for the regulation of DCX that we observe in our models.

We demonstrate a complex relation between levels of AHN and expression of the immature neuron marker doublecortin in two other models. The chronic CORT model where chronic fluoxetine results in a larger increase in the number of DCX-expressing cells than the number of proliferating precursors as measured by KI67 and the number of surviving neurons as measured by BrdU incorporation. Such an observation is in good agreement with an independent report that reached a similar conclusion (Robinson et al., 2016). The other model where we observe a difference between the number of DCX-expressing cells and levels of neurogenesis is a model of inflammation where DCX levels decrease more and faster than neurogenesis. These results suggest that levels of DCX can be regulated independently of levels of neurogenesis; however, we cannot exclude a lower survival and greater loss of immature neurons generated before or after this BrdU labeling. Such observations confirm our previous findings that levels of DCX decrease dramatically already 24 h after X-irradiation, which induces an acute inflammatory response (Denny et al., 2012) even though most young neurons are not affected by X-irradiation.

Another independent line of evidence showing a complete disconnect between levels of doublecortin and levels of neurogenesis comes from the DCX KO mice that display normal levels of neurogenesis in the absence of any DCX-expressing cells (Dhaliwal et al., 2015). Finally, there is evidence that the maturation of young neurons is partially independent of the proliferation and survival of these cells (Baptista & Andrade, 2018; Kempermann et al., 2015; Plümpe et al., 2006). For example, in rats, the levels of DCX are lower than in mice although the levels of neurogenesis are higher and this discrepancy may be due to a faster maturation of the young neurons in rats than in mice (Snyder et al., 2016).

However, it is important to emphasize that DCX is still exclusively expressed by immature adult-born neurons in the DG. DCX is abolished by two manipulations that suppress AHN: x-ray and GFAP-TK. These results argue against the possibility that DCX in the DG could also come from nonneurogenesis-related processes as has been argued by some authors (Kobayashi et al., 2010).

However, DCX is also expressed outside the neurogenic niches and outside the context of adult neurogenesis (Benedetti et al., 2020; Benedetti & Couillard-Despres, 2022; Bonfanti & Nacher, 2012; Bonfanti & Seki, 2021; Coviello et al., 2021; Feliciano et al., 2015; Gomez-Climent et al., 2011; Palazzo et al., 2018; Piumatti et al., 2018;

10981063, 2023, 10, Downloaded from https://onlinelibrary.wiley.com/doi/10.1002/hipo.23568 by Université de Versailles-Saint-Quentin-en-Yvelines, Wiley Online Library on [15/11/2023]. See the Terms and Conditions (https://onlinelibrary.wiley.com/terms-and-conditions) on Wiley Online Library for rules of use; OA articles are governed by the applicable Creative Commons License

Rotheneichner et al., 2018; Sorrells et al., 2019; Vadodaria et al., 2017). We also confirmed in GFAP-TK+ treated-fluoxetine mice, in which AHN is arrested, that DCX is still detected in the piriform cortex (data not shown). Actually, DCX is often found in postmitotic immature neurons in the piriform cortex (and other areas), where the marker is known to wane as postmitotic precursors mature into neurons. Overall, whether related to neurogenesis or not, DCX expression in the adult brain appears to reflect neuronal immaturity.

4.2 | Human neurogenesis

Recent reports have questioned whether AHN occurs in the adult human hippocampus and to what extent (Boldrini et al., 2018; Boldrini et al., 2019a; Moreno-Jiménez et al., 2019; Sorrells et al., 2018; Tartt et al., 2018; Toda et al., 2019). The problem is the most acute in humans, where it is difficult if not impossible to assess the survival of young neurons because lineage studies and label retention studies with BrdU or retroviruses are mostly impossible. Therefore, most human studies have relied on a few markers of immature neurons, such as DCX, to quantify neurogenesis. For example, in the DG of adult healthy humans or Alzheimer patients (Moreno-Jiménez et al., 2019) observed a relative abundance of DCX + immature neurons. In contrast, Sorrells et al. found rare DCX+ cells between 7 and 13 years of age which led these authors to suggest that hippocampal neurogenesis ends in childhood (Sorrells et al., 2018). This problem of quantification is complicated by the fact that these groups used different fixing and staining conditions. In addition, postmortem intervals were highly variable, which has been shown to impact DCX detection (Verwer et al., 2007). Interestingly, in a recent report (W. Wang et al., 2022), Wang and colleagues investigate why the previous study (Franjic et al., 2022) from Franjic failed to detect immature neurons. Analyzing the snRNA-seq data, they found that there is an increase of neuroinflammation signature which may explain why immature neurons could not be found in those samples (Liu, 2022). Finally, levels of stress, inflammation, or other health conditions that may impact neurogenesis are not always well known before the death of the individual. As we have shown in the current study, these factors may have large impacts on the number of DCX-expressing cells and may explain at least in part the current controversy about levels of neurogenesis in the adult human brain (Boldrini et al., 2018; Kempermann et al., 2015; Sorrells et al., 2018; Spalding et al., 2013). Single-cell RNA sequencing strategies may circumvent some of these problems because they do not rely on only a few markers to identify immature neurons. Indeed, Zhou et al. recently identified a rather large number of putative immature neurons in the adult human DG by relying on their transcriptomics signature (Zhou et al., 2022).

In summary, we have shown a complex relation between levels of AHN and expression of the immature neuron marker doublecortin. Although the functional significance of this regulation remains unknown, we hope that our study will provide a cautionary reminder for researchers interested in quantifying neurogenesis in humans, emphasizing the importance of using multiple markers to assess the various stages of the neurogenesis process.

AUTHOR CONTRIBUTIONS

René Hen, Indira Mendez-David, and Denis Joseph David conceived, planned, and oversaw the study. Jean-Martin Beaulieu provided key reagents (β-arrestin-1 ± line). Indira Mendez-David, Denis Joseph David, Claudine Deloménie, and Laurent Tritchler performed the experiments. Indira Mendez-David, Denis Joseph David, and Claudine Deloménie analyzed the data. René Hen, Indira Mendez-David, and Denis Joseph David wrote the paper. Emmanuelle Corruble, Romain Colle, Alain Michel Gardier, Claudine Deloménie, and Jean-Martin Beaulieu assisted in revising the manuscript. Indira Mendez-David and Denis Joseph David obtained funding and resource used in the experiments.

ACKNOWLEDGMENTS

The authors kindly thank Dr H. Cameron (NIMH/NIH) for supplying the GFAP-TK mice (license agreement L-O 15-2015/0 between the National Institutes of Health and Université Paris-Sud). The authors also thank I. Pavlova and the C. Denny's lab for confocal acquisition (Columbia Univ.), V. Domergue and the staff of the animal care facility (UMS-IPSIT Animex, Université Paris-Saclay, Orsay, France) for their technical support. The authors thank Emy Ponsardin et Morgane Pitel (UMS-IPSIT ACTAGen, Université Paris-Saclay, Orsay, France) for her technical support on qPCR. This work was supported Young Investigator Award 2017 to Indira Mendez-Dav and Fondation Pierre Deniker pour la Recherche et la Prévention en Santé Mentale.

CONFLICT OF INTEREST STATEMENT

Denis Joseph David serves as a consultant for Lundbeck Inc and receives compensation from Lundbeck.

DATA AVAILABILITY STATEMENT

The data that support the findings of this study are available from the corresponding author upon reasonable request.

ORCID

Indira Mendez-David https://orcid.org/0000-0001-9759-0833
Denis Joseph David https://orcid.org/0000-0002-0506-6688
Claudine Deloménie https://orcid.org/0000-0002-6326-966X
Laurent Tritchler https://orcid.org/0000-0002-7041-0764
Jean-Martin Beaulieu https://orcid.org/0000-0002-0446-7447
Romain Colle https://orcid.org/0000-0002-2549-4495
Emmanuelle Corruble https://orcid.org/0000-0002-9441-6079
Alain Michel Gardier https://orcid.org/0000-0002-0320-4880
René Hen https://orcid.org/0000-0002-7763-4162

REFERENCES

Anacker, C., Luna, V. M., Stevens, G. S., Millette, A., Shores, R., Jimenez, J. C., Chen, B., & Hen, R. (2018). Hippocampal neurogenesis confers stress resilience by inhibiting the ventral dentate gyrus.

10981063, 2023, 10, Downloaded from https://onlinelibrary.wiley.com/doi/10.1002/hipo.23568 by Université de Versailles-Saint-Quentin-en-Yvelines, Wiley Online Library on [15/11/2023]. See the Terms and Conditions (https://onlinelibrary.wiley.com/terms-and-conditions) on Wiley Online Library for rules of use; OA articles are governed by the applicable Creative Commons License

Nature, *559*(7712), 98–102. https://doi.org/10.1038/s41586-018-0262-4

Asth, L., Ruzza, C., Malfacini, D., Medeiros, I., Guerrini, R., Zaveri, N. T., Gavioli, E. C., & Calo', G. (2016). Beta-arrestin 2 rather than G protein efficacy determines the anxiolytic-versus antidepressant-like effects of nociceptin/orphanin FQ receptor ligands. *Neuropharmacology*, *105*, 434–442. https://doi.org/10.1016/j.neuropharm.2016.02.003

Baptista, P., & Andrade, J. P. (2018). Adult hippocampal neurogenesis: Regulation and possible functional and clinical correlates. *Frontiers in Neuroanatomy*, *12*, 44. https://doi.org/10.3389/fnana.2018.00044

Beaulieu, J. M., Marion, S., Rodriguiz, R. M., Medvedev, I. O., Sotnikova, T. D., Ghisi, V., Wetsel, W. C., Lefkowitz, R. J., Gainetdinov, R. R., & Caron, M. G. (2008). A beta-arrestin 2 signaling complex mediates lithium action on behavior. *Cell*, *132*(1), 125–136. https://doi.org/10.1016/j.cell.2007.11.041

Benedetti, B., & Couillard-Despres, S. (2022). Why would the brain need dormant neuronal precursors? *Frontiers in Neuroscience*, *16*, 877167. https://doi.org/10.3389/fnins.2022.877167

Benedetti, B., Dannehl, D., König, R., Coviello, S., Kreutzer, C., Zaunmair, P., Jakubecova, D., Weiger, T. M., Aigner, L., Nacher, J., Engelhardt, M., & Couillard-Després, S. (2020). Functional integration of neuronal precursors in the adult murine piriform cortex. *Cerebral Cortex*, *30*(3), 1499–1515. https://doi.org/10.1093/cercor/bhz181

Bohn, L. M., & Schmid, C. L. (2010). Serotonin receptor signaling and regulation via beta-arrestins. *Critical Reviews in Biochemistry and Molecular Biology*, *45*(6), 555–566. https://doi.org/10.3109/10409238.2010.516741

Boldrini, M., Fulmore, C. A., Tartt, A. N., Simeon, L. R., Pavlova, I., Poposka, V., Rosoklija, G. B., Stankov, A., Arango, V., Dwork, A. J., Hen, R., & Mann, J. J. (2018). Human hippocampal neurogenesis persists throughout aging. *Cell Stem Cell*, *22*(4), 589–599.e5. https://doi.org/10.1016/j.stem.2018.03.015

Boldrini, M., Galfalvy, H., Dwork, A. J., Rosoklija, G. B., Trencevska-Ivanovska, I., Pavlovski, G., Hen, R., Arango, V., & Mann, J. J. (2019). Resilience is associated with larger dentate gyrus, while suicide decedents with major depressive disorder have fewer granule neurons. *Biological Psychiatry*, *85*(10), 850–862. https://doi.org/10.1016/j.biopsych.2018.12.022

Bonfanti, L., & Nacher, J. (2012). New scenarios for neuronal structural plasticity in non-neurogenic brain parenchyma: The case of cortical layer II immature neurons. *Progress in Neurobiology*, *98*(1), 1–15. https://doi.org/10.1016/j.pneurobio.2012.05.002

Bonfanti, L., & Seki, T. (2021). The PSA-NCAM-positive "immature" neurons: An old discovery providing new vistas on brain structural plasticity. *Cell*, *10*(10), 2542. https://doi.org/10.3390/cells10102542

Burghardt, N. S., Park, E. H., Hen, R., & Fenton, A. A. (2012). Adult-born hippocampal neurons promote cognitive flexibility in mice. *Hippocampus*, *22*(9), 1795–1808. https://doi.org/10.1002/hipo.22013

Chugh, D., Nilsson, P., Afjei, S. A., Bakochi, A., & Ekdahl, C. T. (2013). Brain inflammation induces post-synaptic changes during early synapse formation in adult-born hippocampal neurons. *Experimental Neurology*, *250*, 176–188. https://doi.org/10.1016/j.expneurol.2013.09.005

Coviello, S., Benedetti, B., Jakubecova, D., Belles, M., Klimczak, P., Gramuntell, Y., Couillard-Despres, S., & Nacher, J. (2021). PSA depletion induces the differentiation of immature neurons in the piriform cortex of adult mice. *International Journal of Molecular Sciences*, *22*(11), 5733. https://doi.org/10.3390/ijms22115733

David, D. J., Samuels, B. A., Rainer, Q., Wang, J. W., Marsteller, D., Mendez, I., Drew, M., Craig, D. A., Guiard, B. P., Guilloux, J. P., Artymyshyn, R. P., Gardier, A. M., Gerald, C., Antonijevic, I. A., Leonardo, E. D., & Hen, R. (2009). Neurogenesis-dependent and -independent effects of fluoxetine in an animal model of anxiety/depression. *Neuron*, *62*(4), 479–493. https://doi.org/10.1016/j.neuron.2009.04.017

Denny, C. A., Burghardt, N. S., Schachter, D. M., Hen, R., & Drew, M. R. (2012). 4- to 6-week-old adult-born hippocampal neurons influence novelty-evoked exploration and contextual fear conditioning. *Hippocampus*, *22*(5), 1188–1201. https://doi.org/10.1002/hipo.20964

Dhaliwal, J., Xi, Y., Bruel-Jungerman, E., Germain, J., Francis, F., & Lagace, D. C. (2015). Doublecortin (DCX) is not essential for survival and differentiation of newborn neurons in the adult mouse dentate gyrus. *Frontiers in Neuroscience*, *9*, 494. https://doi.org/10.3389/fnins.2015.00494

Diaz, S. L., Doly, S., Narboux-Nême, N., Fernández, S., Mazot, P., Banas, S. M., … Maroteaux, L. (2012). 5-HT(2B) receptors are required for serotonin-selective antidepressant actions. *Molecular Psychiatry*, *17*(2), 154–163. https://doi.org/10.1038/mp.2011.159

Dwivedi, Y. (2013). microRNAs as biomarker in depression pathogenesis. *Annals of Psychiatry and Mental Health*, *1*(1), 1003.

Dwivedi, Y. (2014). Emerging role of microRNAs in major depressive disorder: Diagnosis and therapeutic implications. *Dialogues in Clinical Neuroscience*, *16*(1), 43–61.

Encinas, J. M., Vaahtokari, A., & Enikolopov, G. (2006). Fluoxetine targets early progenitor cells in the adult brain. *Proceedings of the National Academy of Sciences of the United States of America*, *103*(21), 8233–8238. https://doi.org/10.1073/pnas.0601992103

Evangelisti, C., Florian, M. C., Massimi, I., Dominici, C., Giannini, G., Galardi, S., Buè, M. C., Massalini, S., McDowell, H. P., Messi, E., Gulino, A., Giulia Farace, M., & Ciafre, S. A. (2009). MiR-128 up-regulation inhibits reelin and DCX expression and reduces neuroblastoma cell motility and invasiveness. *The FASEB Journal*, *23*(12), 4276–4287. https://doi.org/10.1096/fj.09-134965

Faye, C., Hen, R., Guiard, B. P., Denny, C. A., Gardier, A. M., Mendez-David, I., & David, D. J. (2019). Rapid anxiolytic effects of RS67333, a serotonin type 4 receptor agonist, and diazepam, a benzodiazepine, are mediated by projections from the prefrontal cortex to the dorsal raphe nucleus. *Biological Psychiatry*, *87*, 514–525. https://doi.org/10.1016/j.biopsych.2019.08.009

Feliciano, D. M., Bordey, A., & Bonfanti, L. (2015). Noncanonical sites of adult neurogenesis in the mammalian brain. *Cold Spring Harbor Perspectives in Biology*, *7*(10), a018846. https://doi.org/10.1101/cshperspect.a018846

Flor-Garcia, M., Terreros-Roncal, J., Moreno-Jimenez, E. P., Avila, J., Rabano, A., & Llorens-Martin, M. (2020). Unraveling human adult hippocampal neurogenesis. *Nature Protocols*, *15*, 668–693. https://doi.org/10.1038/s41596-019-0267-y

Franjic, D., Skarica, M., Ma, S., Arellano, J. I., Tebbenkamp, A. T. N., Choi, J., Xu, C., Li, Q., Morozov, Y. M., Andrijevic, D., Vrselja, Z., Spajic, A., Santpere, G., Li, M., Zhang, S., Liu, Y., Spurrier, J., Zhang, L., Gudelj, I., … Sestan, N. (2022). Transcriptomic taxonomy and neurogenic trajectories of adult human, macaque, and pig hippocampal and entorhinal cells. *Neuron*, *110*(3), 452–469.e14. https://doi.org/10.1016/j.neuron.2021.10.036

Franklin, K. B. J., & Paxinos, G. (2007). *The mouse brain in stereotaxic coordinates* (3rd ed.). Academic Press.

Gomez-Climent, M. A., Hernandez-Gonzalez, S., Shionoya, K., Belles, M., Alonso-Llosa, G., Datiche, F., & Nacher, J. (2011). Olfactory bulbectomy, but not odor conditioned aversion, induces the differentiation of immature neurons in the adult rat piriform cortex. *Neuroscience*, *181*, 18–27. https://doi.org/10.1016/j.neuroscience.2011.03.004

Hagihara, H., Murano, T., Ohira, K., Miwa, M., Nakamura, K., & Miyakawa, T. (2019). Expression of progenitor cell/immature neuron markers does not present definitive evidence for adult neurogenesis. *Molecular Brain*, *12*(1), 108. https://doi.org/10.1186/s13041-019-0522-8

Hellemans, J., Mortier, G., De Paepe, A., Speleman, F., & Vandesompele, J. (2007). qBase relative quantification framework and software for management and automated analysis of real-time quantitative PCR data. *Genome Biology*, *8*(2), R19. https://doi.org/10.1186/gb-2007-8-2-r19

Jin, J., Kim, S. N., Liu, X., Zhang, H., Zhang, C., Seo, J. S., Kim, Y., & Sun, T. (2016). miR-17-92 cluster regulates adult hippocampal neurogenesis,

10981063, 2023, 10, Downloaded from https://onlinelibrary.wiley.com/doi/10.1002/hipo.23568 by Université de Versailles-Saint-Quentin-en-Yvelines, Wiley Online Library on [15/11/2023]. See the Terms and Conditions (https://onlinelibrary.wiley.com/terms-and-conditions) on Wiley Online Library for rules of use; OA articles are governed by the applicable Creative Commons License

anxiety, and depression. *Cell Reports*, *16*(6), 1653–1663. https://doi.org/10.1016/j.celrep.2016.06.101

Kempermann, G., Gast, D., Kronenberg, G., Yamaguchi, M., & Gage, F. H. (2003). Early determination and long-term persistence of adult-generated new neurons in the hippocampus of mice. *Development*, *130*(2), 391–399. https://doi.org/10.1242/dev.00203

Kempermann, G., Song, H., & Gage, F. H. (2015). Neurogenesis in the adult hippocampus. *Cold Spring Harbor Perspectives in Biology*, *7*(9), a018812. https://doi.org/10.1101/cshperspect.a018812

Klempin, F., Kronenberg, G., Cheung, G., Kettenmann, H., & Kempermann, G. (2011). Properties of doublecortin-(DCX)-expressing cells in the piriform cortex compared to the neurogenic dentate gyrus of adult mice. *PLoS One*, *6*(10), e25760. https://doi.org/10.1371/journal.pone.0025760

Kobayashi, K., Ikeda, Y., Sakai, A., Yamasaki, N., Haneda, E., Miyakawa, T., & Suzuki, H. (2010). Reversal of hippocampal neuronal maturation by serotonergic antidepressants. *Proceedings of the National Academy of Sciences of the United States of America*, *107*(18), 8434–8439. https://doi.org/10.1073/pnas.0912690107

Kohler, S. J., Williams, N. I., Stanton, G. B., Cameron, J. L., & Greenough, W. T. (2011). Maturation time of new granule cells in the dentate gyrus of adult macaque monkeys exceeds six months. *Proceedings of the National Academy of Sciences of the United States of America*, *108*(25), 10326–10331. https://doi.org/10.1073/pnas.1017099108

Kremer, T., Jagasia, R., Herrmann, A., Matile, H., Borroni, E., Francis, F., Kuhn, H. G., & Czech, C. (2013). Analysis of adult neurogenesis: Evidence for a prominent "non-neurogenic" DCX-protein pool in rodent brain. *PLoS One*, *8*(5), e59269. https://doi.org/10.1371/journal.pone.0059269

Lino de Oliveira, C., Bolzan, J. A., Surget, A., & Belzung, C. (2020). Do antidepressants promote neurogenesis in adult hippocampus? A systematic review and meta-analysis on naive rodents. *Pharmacology & Therapeutics*, *210*, 107515. https://doi.org/10.1016/j.pharmthera.2020.107515

Liu, H. K. (2022). Human adult hippocampal neurogenesis is back, again? *Cell Research*, *32*, 793–794. https://doi.org/10.1038/s41422-022-00698-8

Ma, Z., Zang, T., Birnbaum, S. G., Wang, Z., Johnson, J. E., Zhang, C. L., & Parada, L. F. (2017). TrkB dependent adult hippocampal progenitor differentiation mediates sustained ketamine antidepressant response. *Nature Communications*, *8*(1), 1668. https://doi.org/10.1038/s41467-017-01709-8

Malberg, J. E., Eisch, A. J., Nestler, E. J., & Duman, R. S. (2000). Chronic antidepressant treatment increases neurogenesis in adult rat hippocampus. *The Journal of Neuroscience*, *20*(24), 9104–9110.

Mendez-David, I., David, D. J., Darcet, F., Wu, M. V., Kerdine-Romer, S., Gardier, A. M., & Hen, R. (2014). Rapid anxiolytic effects of a 5-HT (4) receptor agonist are mediated by a neurogenesis-independent mechanism. *Neuropsychopharmacology*, *39*(6), 1366–1378. https://doi.org/10.1038/npp.2013.332

Mendez-David, I., Guilloux, J. P., Papp, M., Tritschler, L., Mocaer, E., Gardier, A. M., Bretin, S., & David, D. J. (2017). S 47445 produces antidepressant- and anxiolytic-like effects through neurogenesis dependent and independent mechanisms. *Frontiers in Pharmacology*, *8*, 462. https://doi.org/10.3389/fphar.2017.00462

Mendez-David, I., Schofield, R., Tritschler, L., Colle, R., Guilloux, J. P., Gardier, A. M., … David, D. J. (2022). Reviving through human hippocampal newborn neurons. *Encephale*, *48*(2), 179–187. https://doi.org/10.1016/j.encep.2021.09.001

Moreno-Jiménez, E. P., Flor-García, M., Terreros-Roncal, J., Rábano, A., Cafini, F., Pallas-Bazarra, N., Ávila, J., & Llorens-Martín, M. (2019). Adult hippocampal neurogenesis is abundant in neurologically healthy subjects and drops sharply in patients with Alzheimer's disease. *Nature Medicine*, *25*(4), 554–560. https://doi.org/10.1038/s41591-019-0375-9

Ngwenya, L. B., Heyworth, N. C., Shwe, Y., Moore, T. L., & Rosene, D. L. (2015). Age-related changes in dentate gyrus cell numbers, neurogenesis, and associations with cognitive impairments in the rhesus monkey. *Frontiers in Systems Neuroscience*, *9*, 102. https://doi.org/10.3389/fnsys.2015.00102

Ohira, K., Hagihara, H., Miwa, M., Nakamura, K., & Miyakawa, T. (2019). Fluoxetine-induced dematuration of hippocampal neurons and adult cortical neurogenesis in the common marmoset. *Molecular Brain*, *12*(1), 69. https://doi.org/10.1186/s13041-019-0489-5

Ohira, K., Kobayashi, K., Toyama, K., Nakamura, H. K., Shoji, H., Takao, K., Takeuchi, R., Yamaguchi, S., Kataoka, M., Otsuka, S., Takahashi, M., & Miyakawa, T. (2013). Synaptosomal-associated protein 25 mutation induces immaturity of the dentate granule cells of adult mice. *Molecular Brain*, *6*, 12. https://doi.org/10.1186/1756-6606-6-12

Opal, M. D., Klenotich, S. C., Morais, M., Bessa, J., Winkle, J., Doukas, D., Kay, L. J., Sousa, N., & Dulawa, S. M. (2014). Serotonin 2C receptor antagonists induce fast-onset antidepressant effects. *Molecular Psychiatry*, *19*(10), 1106–1114. https://doi.org/10.1038/mp.2013.144

Palazzo, O., La Rosa, C., Piumatti, M., & Bonfanti, L. (2018). Do large brains of long-living mammals prefer non-newly generated, immature neurons? *Neural Regeneration Research*, *13*(4), 633–634. https://doi.org/10.4103/1673-5374.230282

Piumatti, M., Palazzo, O., La Rosa, C., Crociara, P., Parolisi, R., Luzzati, F., Lévy, F., & Bonfanti, L. (2018). Non-newly generated, "immature" neurons in the sheep brain are not restricted to cerebral cortex. *The Journal of Neuroscience*, *38*(4), 826–842. https://doi.org/10.1523/JNEUROSCI.1781-17.2017

Plümpe, T., Ehninger, D., Steiner, B., Klempin, F., Jessberger, S., Brandt, M., Römer, B., Rodriguez, G. R., Kronenberg, G., & Kempermann, G. (2006). Variability of doublecortin-associated dendrite maturation in adult hippocampal neurogenesis is independent of the regulation of precursor cell proliferation. *BMC Neuroscience*, *7*, 77. https://doi.org/10.1186/1471-2202-7-77

Pytka, K., Głuch-Lutwin, M., Żmudzka, E., Sałaciak, K., Siwek, A., Niemczyk, K., … Marona, H. (2018). HBK-17, a 5-HT1A receptor ligand with anxiolytic-like activity, preferentially activates ss-arrestin signaling. *Frontiers in Pharmacology*, *9*, 1146. https://doi.org/10.3389/fphar.2018.01146

Rainer, Q., Xia, L., Guilloux, J. P., Gabriel, C., Mocaër, E., Hen, R., Enhamre, E., Gardier, A. M., & David, D. J. (2012). Beneficial behavioural and neurogenic effects of agomelatine in a model of depression/anxiety. *The International Journal of Neuropsychopharmacology*, *15*(3), 321–335. https://doi.org/10.1017/S1461145711000356

Robinson, S. A., Brookshire, B. R., & Lucki, I. (2016). Corticosterone exposure augments sensitivity to the behavioral and neuroplastic effects of fluoxetine in C57BL/6 mice. *Neurobiology of Stress*, *3*, 34–42. https://doi.org/10.1016/j.ynstr.2015.12.005

Rotheneichner, P., Belles, M., Benedetti, B., König, R., Dannehl, D., Kreutzer, C., Zaunmair, P., Engelhardt, M., Aigner, L., Nacher, J., & Couillard-Despres, S. (2018). Cellular plasticity in the adult murine piriform cortex: Continuous maturation of dormant precursors into excitatory neurons. *Cerebral Cortex*, *28*(7), 2610–2621. https://doi.org/10.1093/cercor/bhy087

Sagi, Y., Medrihan, L., George, K., Barney, M., McCabe, K. A., & Greengard, P. (2019). Emergence of 5-HT5A signaling in parvalbumin neurons mediates delayed antidepressant action. *Molecular Psychiatry*, *25*, 1191–1201. https://doi.org/10.1038/s41380-019-0379-3

Samuels, B. A., Mendez-David, I., Faye, C., David, S. A., Pierz, K. A., Gardier, A. M., … David, D. J. (2016). Serotonin 1A and serotonin 4 receptors: Essential mediators of the neurogenic and behavioral actions of antidepressants. *The Neuroscientist*, *22*(1), 26–45. https://doi.org/10.1177/1073858414561303

Sanai, N., Nguyen, T., Ihrie, R. A., Mirzadeh, Z., Tsai, H. H., Wong, M., Gupta, N., Berger, M. S., Huang, E., Garcia-Verdugo, J. M.,

10981063, 2023, 10, Downloaded from https://onlinelibrary.wiley.com/doi/10.1002/hipo.23568 by Université de Versailles-Saint-Quentin-en-Yvelines, Wiley Online Library on [15/11/2023]. See the Terms and Conditions (https://onlinelibrary.wiley.com/terms-and-conditions) on Wiley Online Library for rules of use; OA articles are governed by the applicable Creative Commons License

Rowitch, D. H., & Alvarez-Buylla, A. (2011). Corridors of migrating neurons in the human brain and their decline during infancy. *Nature*, *478*(7369), 382–386. https://doi.org/10.1038/nature10487

Santarelli, L., Saxe, M., Gross, C., Surget, A., Battaglia, F., Dulawa, S., Weisstaub, N., Lee, J., Duman, R., Arancio, O., Belzung, C., & Hen, R. (2003). Requirement of hippocampal neurogenesis for the behavioral effects of antidepressants. *Science*, *301*(5634), 805–809. https://doi.org/10.1126/science.1083328

Saxe, M. D., Battaglia, F., Wang, J. W., Malleret, G., David, D. J., Monckton, J. E., Garcia, A. D. R., Sofroniew, M. V., Kandel, E. R., Santarelli, L., Hen, R., & Drew, M. R. (2006). Ablation of hippocampal neurogenesis impairs contextual fear conditioning and synaptic plasticity in the dentate gyrus. *Proceedings of the National Academy of Sciences of the United States of America*, *103*(46), 17501–17506. https://doi.org/10.1073/pnas.0607207103

Schloesser, R. J., Manji, H. K., & Martinowich, K. (2009). Suppression of adult neurogenesis leads to an increased hypothalamo-pituitary-adrenal axis response. *Neuroreport*, *20*(6), 553–557. https://doi.org/10.1097/WNR.0b013e3283293e59

Snyder, J. S. (2019). Recalibrating the relevance of adult neurogenesis. *Trends in Neurosciences*, *42*(3), 164–178. https://doi.org/10.1016/j.tins.2018.12.001

Snyder, J. S., Grigereit, L., Russo, A., Seib, D. R., Brewer, M., Pickel, J., & Cameron, H. A. (2016). A transgenic rat for specifically inhibiting adult neurogenesis. *eNeuro*, *3*(3), ENEURO.0064-16.2016. https://doi.org/10.1523/ENEURO.0064-16.2016

Snyder, J. S., Soumier, A., Brewer, M., Pickel, J., & Cameron, H. A. (2011). Adult hippocampal neurogenesis buffers stress responses and depressive behaviour. *Nature*, *476*(7361), 458–461. https://doi.org/10.1038/nature10287

Sorrells, S. F., Paredes, M. F., Cebrian-Silla, A., Sandoval, K., Qi, D., Kelley, K. W., James, D., Mayer, S., Chang, J., Auguste, K. I., Chang, E. F., Gutierrez, A. J., Kriegstein, A. R., Mathern, G. W., Oldham, M. C., Huang, E. J., Garcia-Verdugo, J. M., Yang, Z., & Alvarez-Buylla, A. (2018). Human hippocampal neurogenesis drops sharply in children to undetectable levels in adults. *Nature*, *555*(7696), 377–381. https://doi.org/10.1038/nature25975

Sorrells, S. F., Paredes, M. F., Velmeshev, D., Herranz-Pérez, V., Sandoval, K., Mayer, S., Chang, E. F., Insausti, R., Kriegstein, A. R., Rubenstein, J. L., Manuel Garcia-Verdugo, J., Huang, E. J., & Alvarez-Buylla, A. (2019). Immature excitatory neurons develop during adolescence in the human amygdala. *Nature Communications*, *10*(1), 2748. https://doi.org/10.1038/s41467-019-10765-1

Spalding, K. L., Bergmann, O., Alkass, K., Bernard, S., Salehpour, M., Huttner, H. B., Boström, E., Westerlund, I., Vial, C., Buchholz, B. A., Possnert, G., Mash, D. C., Druid, H., & Frisén, J. (2013). Dynamics of hippocampal neurogenesis in adult humans. *Cell*, *153*(6), 1219–1227. https://doi.org/10.1016/j.cell.2013.05.002

Svenningsson, P., Chergui, K., Rachleff, I., Flajolet, M., Zhang, X., El Yacoubi, M., Vaugeois, J. M., Nomikos, G. G., & Greengard, P. (2006). Alterations in 5-HT1B receptor function by p11 in depression-like states. *Science*, *311*(5757), 77–80. https://doi.org/10.1126/science.1117571

Tartt, A. N., Fulmore, C. A., Liu, Y., Rosoklija, G. B., Dwork, A. J., Arango, V., Hen, R., Mann, J. J., & Boldrini, M. (2018). Considerations for assessing the extent of hippocampal neurogenesis in the adult and aging human brain. *Cell Stem Cell*, *23*(6), 782–783. https://doi.org/10.1016/j.stem.2018.10.025

Toda, T., Parylak, S. L., Linker, S. B., & Gage, F. H. (2019). The role of adult hippocampal neurogenesis in brain health and disease. *Molecular Psychiatry*, *24*(1), 67–87. https://doi.org/10.1038/s41380-018-0036-2

Vadodaria, K. C., Yanpallewar, S. U., Vadhvani, M., Toshniwal, D., Liles, L. C., Rommelfanger, K. S., Weinshenker, D., & Vaidya, V. A. (2017). Noradrenergic regulation of plasticity marker expression in the adult rodent piriform cortex. *Neuroscience Letters*, *644*, 76–82. https://doi.org/10.1016/j.neulet.2017.02.060

Verwer, R. W., Sluiter, A. A., Balesar, R. A., Baayen, J. C., Noske, D. P., Dirven, C. M., Wouda, J., van Dam, A. M., Lucassen, P. J., & Swaab, D. F. (2007). Mature astrocytes in the adult human neocortex express the early neuronal marker doublecortin. *Brain*, *130*(Pt 12), 3321–3335. https://doi.org/10.1093/brain/awm264

Wang, J. W., David, D. J., Monckton, J. E., Battaglia, F., & Hen, R. (2008). Chronic fluoxetine stimulates maturation and synaptic plasticity of adult-born hippocampal granule cells. *The Journal of Neuroscience*, *28*(6), 1374–1384. https://doi.org/10.1523/JNEUROSCI.3632-07.2008

Wang, W., Wang, M., Yang, M., Zeng, B., Qiu, W., Ma, Q., Jing, X., Zhang, Q., Wang, B., Yin, C., Zhang, J., Ge, Y., Lu, Y., Ji, W., Wu, Q., Ma, C., & Wang, X. (2022). Transcriptome dynamics of hippocampal neurogenesis in macaques across the lifespan and aged humans. *Cell Research*, *32*(8), 729–743. https://doi.org/10.1038/s41422-022-00678-y

Zhou, Y., Su, Y., Li, S., Kennedy, B. C., Zhang, D. Y., Bond, A. M., Sun, Y., Jacob, F., Lu, L., Hu, P., Viaene, A. N., Helbig, I., Kessler, S. K., Lucas, T., Salinas, R. D., Gu, X., Chen, H. I., Wu, H., Kleinman, J. E., … Song, H. (2022). Molecular landscapes of human hippocampal immature neurons across lifespan. *Nature*, *607*(7919), 527–533. https://doi.org/10.1038/s41586-022-04912-w

SUPPORTING INFORMATION

Additional supporting information can be found online in the Supporting Information section at the end of this article.

How to cite this article: Mendez-David, I., David, D. J., Deloménie, C., Tritchler, L., Beaulieu, J.-M., Colle, R., Corruble, E., Gardier, A. M., & Hen, R. (2023). A complex relation between levels of adult hippocampal neurogenesis and expression of the immature neuron marker doublecortin. *Hippocampus*, *33*(10), 1075–1093. https://doi.org/10.1002/hipo.23568

10981063, 2023, 10, Downloaded from https://onlinelibrary.wiley.com/doi/10.1002/hipo.23568 by Université de Versailles-Saint-Quentin-en-Yvelines, Wiley Online Library on [15/11/2023]. See the Terms and Conditions (https://onlinelibrary.wiley.com/terms-and-conditions) on Wiley Online Library for rules of use; OA articles are governed by the applicable Creative Commons License